

# **Regulation of receptors Siglec-11 and Siglec-15 by microRNAs and their overall effect on glioblastoma.**

**By Dema Al-Azzawi**

**Supervisory team:**

**Dr Shoib Siddiqui**

**Dr Maria Braoudaki**

**Dr Lisa Lione**

Submitted to the University of Hertfordshire in partial fulfilment of the requirement of the degree of Masters by Research

School of Life and Medical Sciences  
University of Hertfordshire

Date: August 2022

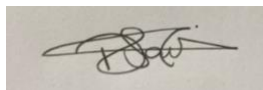
## DECLARATION

I declare that:

- (a) all the work described in this report has been carried out by me – and all the results (including any survey findings, etc.) given herein were first obtained by me – except where I may have given due acknowledgement to others;
- (b) all the prose in this report has been written by me in my own words, except where I may have given due acknowledgement to others and used quotation marks, and except also for occasional brief phrases of no special significance which may be taken from other people’s work without such acknowledgement and use of quotation marks;
- (c) all the figures and diagrams in this report have been devised and produced by me, except where I may have given due acknowledgement to others.
- (d) the project has been spell and grammar checked.

I understand that if I have not complied with the above statements, I may be deemed to have failed the project assessment, and/or I may have some other penalty imposed upon me by the Board of Examiners.

**Signed**



**Date** 19/08/2022

**Name**

Dema Al-Azzawi

**Programme code** 8LMS0227

# Table of Contents

<b>1. Introduction</b>	
1.1 Overview of Glioblastoma and its Diagnosis	07
1.2 Incidence rates and risk factors	08
1.3 Prognosis and clinical features	10
1.4 Role of immune system in tumour microenvironment	11
1.5 Current therapies	12
1.6 Immunotherapy	14
1.7 Siglecs and sialic acid	16
1.8 Potential treatments	19
1.9 Hypothesis	21
1.9.1 Aims	
1.9.2 Objectives	
<b>2. Methods</b>	
2.1 Bioinformatics	22
2.2 Cell culture	22
2.3 MiRNA isolation	22
2.4 Organic extraction	23
2.5 cDNA synthesis	25
2.6 Quantitative Real time Polymerase Chain Reaction (RT-qPCR)	26
2.7 RT-qPCR with genes	27
2.8 Western blots	29
<b>3. Results</b>	
3.1 Bioinformatic analysis results	31
3.2 RT-qPCR	43
3.3 Western blots	47
<b>4. Discussion</b>	48
<b>5. Conclusion</b>	51
<b>6. Future work</b>	52
<b>7. References</b>	53

# List of Figures and Tables

**Figure 1.** MRI of a patient with a new-onset seizure.

**Figure 2.** Glioblastoma incidence rates normalised by age and gender.

**Figure 3.** Structure of the brain. Image created using biorender.

**Figure 4.** A comparison between a normal human body that expresses Siglec-11 compared to a tumour one. Image from Gepia2.

**Figure 5.** A comparison between a normal human body that expresses Siglec-15 compared to a tumour one. Image from Gepia2.

**Figure 6.** Analysis of various bioinformatic tools to show the similarity of miRNA hits found. Image created using VENNY 2.0.

**Figure 7.** Expression analysis of chosen Siglecs using GEPIA.

**Figure 8.** Overall survival analysis of chosen Siglecs using GEPIA.

**Figure 9.** Linear and log amplification plots from RT-qPCR for hsa-miR-RNU-44, hsa-miR-138-5p, hsa-miR-153 and hsa-miR-107 within the A172 GBM cell line.

**Figure 10.** Linear and log amplification plots from RT-qPCR for Siglec-15 and GAPDH within the A172 GBM cell line.

**Figure 11.** CT values for RT-qPCR results.

**Figure 12.** Western blot results for Siglec-15, *E2F3* and *CDK6*.

**Table 1.** RT reaction mix volumes.

**Table 2.** Condition for RT reaction.

**Table 3.** RT-qPCR reaction mix volumes.

**Table 4.** Conditions for RT-qPCR reaction.

**Table 5.** RT Master Mix without RNase inhibitor components and volumes.

**Table 6.** Conditions for Fast Advanced Master Mix.

**Table 7.** RT-qPCR reaction mix volumes.

**Table 8.** Identification of target miRNA for Siglec-11 and Siglec-15 through bioinformatic analysis.

## Abstract

**Introduction:** Glioblastoma is a fast growing and aggressive type of brain tumour. It is the most common type of brain tumour in adults. Although there are developments in current therapies, patient outcomes remain poor. Therefore, new therapeutic strategies are being developed to improve patient prognosis and treatment outcomes. This study aimed to identify novel therapeutic targets for glioblastomas by understanding how Siglec-11 and Siglec-15 are regulated by microRNAs (miRNAs). Siglecs are cell surface receptor molecules that act as a lectin and bind to nine carbon atom sugar sialic acid. Siglec-11 is an inhibitory siglec that is expressed on microglia in the brain. Siglec-15 is expressed in a variety of cancers, however its presence in brain cancer cells has been elusive. Both Siglec-11 and Siglec-15 upon binding with their ligand generate immune inhibitory signals. Thus, they are assumed to be target for cancer immunotherapy. Although there has been active research on their therapeutic targeting, their gene expression regulation has not been extensively researched. Therefore, the aim of this project is to decipher the gene expression regulation of Siglec-11 and Siglec-15 by miRNAs.

**Methods:** Bioinformatics analysis was performed using different online tools; Targetscan ([https://www.targetscan.org/vert\\_72/](https://www.targetscan.org/vert_72/)), miRSystem (<http://mirsystem.cgm.ntu.edu.tw>), DIANA (<https://diana.e-ce.uth.gr/tools>) and miRwalk (<http://mirwalk.umm.uni-heidelberg.de>) were used to identify which miRNAs are involved in the regulation of both Siglecs. Following this, the expression of specific miRNAs was further validated in A172 glioblastoma cell lines using quantitative real time polymerase chain reaction (RT-qPCR). To do so, RNA extraction was carried out using the Trizol method, whilst miRNA extraction was performed with the mirVANA miRNA isolation kit. RT-qPCR was performed to validate the expression profiles of the following miRNAs: hsa-miR-138-5p, hsa-miR-153 and hsa-miR-107. Another bioinformatics tool GEPIA2 was used to identify the expression and survival of Siglec-11 and Siglec-15 between cancer patients and healthy individuals.

**Results:** The results from the bioinformatic analysis highlighted that the miRNAs that are highly downregulated in cancer; hsa-miR-138-5p, hsa-miR-153 and hsa-miR-107 were heavily downregulated in cancer. The downregulation of hsa-miR-138-5p, hsa-miR-153 and hsa-miR-107 was confirmed by qRT-PCR in glioblastoma cell line A172. The results from GEPIA2 showed that Siglec-11 and Siglec-15 are highly upregulated

in cancer patients as compared to healthy individuals. However, there was no statistical difference in the survival of glioblastoma patients between the high and low expressors of Siglec-11 and Siglec-15. Western blot was carried out for 3 different markers: Siglec-15, *E2F3* and *CDK6*.

**Conclusion:** The expression of the following miRNAs was found to be heavily downregulated in cancer; hsa-miR-138-5p, hsa-miR-153 and hsa-miR-107 indicating that they might manifest tumor suppressor properties. Siglec-11 and Siglec-15 can be used as diagnostic markers and therapeutic targets in glioblastomas as they are regulated by these tumour suppressor miRNAs. However, further functional assays are required to prove the association between these miRNAs and the Siglecs under investigation. Altering miRNA expression levels is regarded to be a possible technique for developing effective cancer therapeutics. A good expression of Siglec-15, *CKD6* and *E2F3* were shown on protein level using western blot in A172 cell line.

# 1. Introduction

## 1.1 Overview of Glioblastoma and its Diagnosis

Glioblastoma (GBM) is a malignant brain tumour which grows diffusely and has several distinct histological features (Preusser, M. et al. 2011). While radiological and clinical tumour features are occasionally included in their classification, current guidelines as per the World Health Organisation (WHO) suggest classification should be primarily based on the distinct histological features of glioblastoma. In cases of high-grade infiltrating astrocytic tumours, these include: hypercellularity, nuclear atypia, and mitotic activity (Aldape, K. et al. 2015). Most primary glioblastomas develop quickly, with only a few days or weeks prior clinical history.

Gliomas are hard to identify early on since the presenting symptoms are often common and may not be severe enough to raise concern of possible glioma diagnosis (e.g., headaches, personality changes and memory loss). And while speech or motor function issues may occur, they are typically not easily recognised. Magnetic resonance imaging (MRI) or computed tomography are frequently used to confirm the diagnosis, and the tumour usually appears as a mass with surrounding edema. Proton magnetic resonance spectroscopy (MRS) can be used to measure metabolite levels and identify a tumour from necrotic regions or benign lesions. *In vivo*, MRS measures the spectra of certain isotopes to identify metabolites such as choline (Cho), creatine (Cr), lactate and lipids. Due to the metabolite levels varying within the brain and among age groups, it was proposed that metabolite ratios, such as Cho/Cr, be measured rather than absolute metabolite concentrations. However, these approaches may be costly and so different diagnostic methods may be required (Jovčevska, I. et al. 2013).

Despite being a histologically homogenous collection of tumours, discoveries in molecular neuropathology have shown that GBM may be divided into clinically significant subgroups that utilise molecular classification methods (Aldape, K. et al. 2015). Microarray studies stemming from the Cancer Genome Project have revealed four characterisable categories of GBM: classical, pro-neural, neural and mesenchymal subgroups. Genetic profiling appears to differentiate tumours that arise from pre-existing low-grade gliomas from those that arise primarily as GBM. Mutations in the isocitrate dehydrogenase (IDH) gene is a distinguishing factor and is an early

alteration in gliomas. It is found in just 5% of primary GBM's and mutations in GBM patients may indicate a better predictive subgroup (Lieberman, F. 2017).

Glioblastoma is characterised by an infiltrative, heterogeneous, ring-enhancing lesion with central necrosis and peritumoral edema on imaging. The deep white matter and the corpus callosum are frequently involved. Although multifocal enhancement is uncommon, smaller satellite regions of enhancement and regional necrosis can occur. Initially, a small non- enhancing or slightly enhancing lesion is observed, but in a few weeks, it transforms into a ring-enhancing, necrotic lesion with peritumoral edema (Alexander, B. et al. 2017). An example of how glioblastoma presents can be seen in Figure 1.

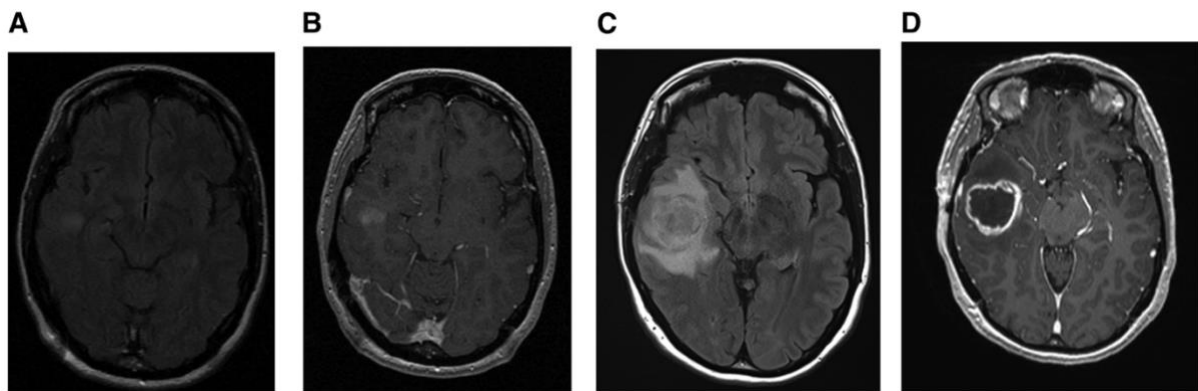


**Figure 1.** MRI of a patient with a new-onset seizure (Alexander, B. et al. 2017). Figure 1A and Figure 1B show a small lesion in the right temporal lobe with no edema and weak enhancement. Figure 1C and Figure 1D are 20-day MR scans that show fast progression to a massive ring-enhancing tumour with a necrotic core and substantial perilesional edema. Glioblastoma was discovered in the pathology report.

The clinical appearance depends on the location and size of the tumour. Focused neurological disorders (aphasia, visual disturbances), seizures, mood and personality disorders, or elevated intracranial pressure symptoms such as headaches or vomiting are all common symptoms of primary glioblastoma (Preusser, M. et al. 2011).

## 1.2 Incidence rates and risk factors

GBM is known as the most common primary brain tumour (Davis, M. et al. 2016). It accounts for 69% of all oligodendroglioma and astrocytic tumour cases (Ohgaki, H. et al.



2007). The annual incidence rate for primary GBM is approximately 3 to 5 new cases per 100,000 individuals (Preusser, M. et al. 2011). Figure 2 shows the glioblastoma incidence rates.

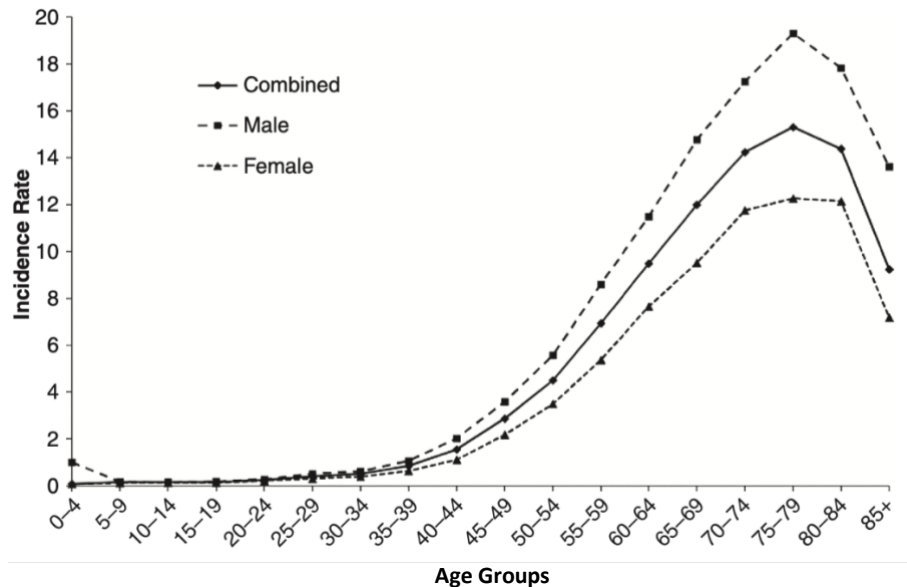


**Figure 2.** Glioblastoma incidence rates normalised by age and gender. The X-axis represents age groups, whereas the Y-axis represents incidence rates. The rates are per 100,000 and age-adjusted to the standard population of the United States in 2000. (Ostrom, Q. et al. 2013).

GBM incidence increase with age, and the median age of diagnosis is 65 years (Birzuic, C. et al. 2020). Younger patients (<56 years old) are more likely to have a cerebellar GBM whilst older patients (62 years old) are more likely to have supratentorial GBM (Tamimi, A. et al. 2017). GBM affects both genders, although they are more common in males, excluding the posterior fossa. It is twice as prevalent in European descendants in comparison to Asian or African descendants (Preusser, M. et al. 2011).

Prior exposure to radiation, immunological factors, lower allergy sensitivity and several nucleotide polymorphisms revealed by genome-wide association studies are all linked to glioblastoma risk. The lower prevalence of glioblastoma in those with asthma and other allergic disorders matches findings from asthma and other allergies-related germline polymorphism in glioblastoma patients compared to controls. Genotypes that enhance asthma risk are linked to a lower risk of being diagnosed with glioblastoma.

Allergy or atopic conditions, such as asthma or eczema, have also been linked to a reduced incidence of glioma diagnosis. Anti-inflammatory medicine usage for <10 years has also been linked to a protective effect against glioblastoma. There is no indication of a link between glioblastoma and lifestyle factors such as smoking, drug use and alcohol intake (Tamimi, A. et al. 2017).

### 1.3 Prognosis and clinical features

The median survival of patients who undergo treatment has risen by more than 15 months. Between 2000 and 2014, individuals who were diagnosed in the United States had an overall 1-year survival rate of 41.4%, which is an increase of 34.4% from 2000-2004 and 44.6% from 2005-2014 (Tan, A. et al. 2020). Advanced age of patients, an insufficient resection and poor performance status are all negative prognostic factors affecting patient survival.

The frontal lobe, multiple lobes (overlapping tumours), temporal and parietal lobes have the highest incidence of GBM in the supratentorial region of the brain (frontal, temporal, parietal, and occipital lobes) (Tamimi, A. et al. 2017).

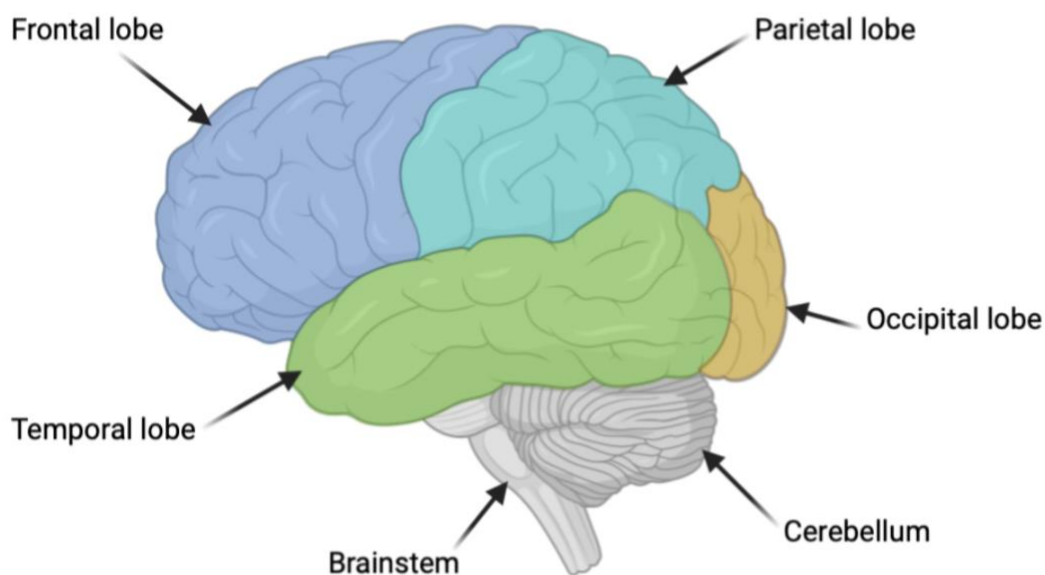


**Figure 3.** Structure of the brain. Image created using biorender.

The clinical features of glioblastoma are generally linked to the functional region of the affected brain. Tumours in specific locations can create noticeable symptoms ranging from numbness, persistent weakness, or vision loss. In these cases, tumour size tends to be smaller on imaging. Mood disorders, memory difficulties and weariness are all indicative of tumours in other parts of the brain. These tumours are often seen in the frontal lobe, temporal lobe or corpus callosum (bundles of myelinated nerve fibres) and are usually bigger when diagnosed (Alexander, B. et al. 2017).

#### **1.4 Role of immune system in a tumour microenvironment**

The blood brain barrier (BBB), which restricts free movement of cells and molecules, and the lack of a classical lymphatic drainage system has allowed the central nervous system (CNS) to be previously seen as an immune-privileged location. Brain tumours, on the other hand, have been known for more than 20 years to trigger antitumour immune responses. Furthermore, inflammatory stimuli provided by brain tumours can activate microglia and damage the BBB. Microglia are the primary effector cells of the innate immune system in the central nervous system and are involved in phagocytosis as well as T-cell activation via antigen presentation (Huang, B. et al. 2017). Both tumour cell invasion and proliferation are aided by microglia. Tumour associated macrophages (TAMs), alongside with central nervous system microglia, can make up to 30% of the tumour mass (Brown, N. et al. 2018). TAMs may be driven into an immunosuppressive M2 phenotype by adjacent astrocytes. This results in the release of chemicals such as TGF- $\beta$ , which subsequently shut off cytotoxic T cells and metalloproteinase (MMP)-14. The release of these chemicals causes a breakdown of the extracellular matrix, thus slowing tumour growth and development. A high CD4+ and low CD8+ T lymphocyte ratio may indicate poor outcomes. Glioblastoma patients had higher amounts of circulating myeloid-derived suppressor cells, which may reduce tumour lymphocyte infiltration even further (Wilcox, J. et al. 2018).

The immune system can distinguish between self and non-self, and continual antigen sampling suggests that certain foreign antigens will inevitably mimic antigens found in the body. It contains mechanisms for slowing down and preventing autoimmunity. Regulatory T cells (T-regs) are used to inhibit immunological activation. Therefore, T-regs are now recognised as a critical regulatory route in tumour tolerance, with a

distinct cell surface profile that includes both CD25 and CD4 expression. Other cell surface indicators, such as the glucocorticoid-induced tumour necrosis factor (GITR) and cytotoxic T-lymphocyte associated antigen 4 (CTLA4) are expressed by regulatory T cells. CTLA4 competes with CD28 for the binding of B7, which is an integral membrane protein found on antigen presenting cells (APCs) (Mc Adam, A. et al. 1998), suppressing T cell activation. Regulatory T cells suppress CD4+/CD8+ T cells and dendritic cells (DCs), resulting in a reduced immunological response (Thomas, A. et al. 2012). Dendritic cells (DCs) are immune system regulators that are best recognised for their capacity to trigger adaptive immunity (Schrami, B. et al. 2015).

The tumour suppressor retinoblastoma (pRB) inhibits cell cycle progression by binding to transcription factors of the E2F family and inhibiting it. The pRB is encoded by the RB gene, is regulated by the cyclin-dependent kinase complex (CDKs). This gene has also been linked to the malignant development of astrocytoma and the deletion of pRB expression has previously been seen in glioblastoma (Tortoso, A. et al. 2000). The tumour suppressor retinoblastoma is normally inactivated in the G1 phase of the cell cycle by Cyclin D/CDK-6 induced phosphorylation, which results in the release of pRB from E2F and the subsequent promotion of cell progression into the S phase. CDKN2B, a CDK inhibitor that is typically inactivated in glioblastoma, forms a complex with CDK6, resulting in the inhibition of CDK activation. This inhibition impacts downstream processes, preventing cell development and the cell cycle advancement through the G1 phase by keeping pRB activated. Inhibiting CDK6 may be a potential chemotherapeutic treatment option for glioblastoma patients with aberrantly produced pRB since the kinase activity is inhibited in the CDK6/Cyclin D complex which inactivates the pRB pathway (Mao, H. et al. 20212).

### **1.5 Current therapies**

The current gold standard glioblastoma treatment is an aggressive combination therapy, involving maximal safe surgical resection, adjuvant radiation, and temozolomide chemotherapy. The diffusely infiltrative nature of gliomas makes surgical resection challenging as tumours often reoccur. Tumour location can also affect surgery success whereby malignant tumours penetrating important brain structures are usual. Following surgery, radiation treatment increases median survival

time from 14 to 36 weeks. The advantages of radiotherapy were first demonstrated using whole brain radiotherapy, but advances in technology, such as field radiation therapy, have significantly increased treatment specificity and minimised the adverse effects associated with whole brain radiotherapy (Lee, D. et al. 2017).

Extensive surgical resection of glioblastoma is challenging as tumours are usually invasive and typically occur in parts of the brain controlling vital bodily functions, such as areas that regulate speech and motor function. Radical resection of the initial tumour mass is largely ineffective due to high tumour invasiveness, and infiltrating tumour cells surrounding the brain, which lead to disease progression or tumour recurrence. Aggressive surgical resection improves results, with patients who have a larger resection having better outcomes. With advancements in surgical and preoperative mapping procedures, more extensive resection can now be achieved while maintaining brain function and quality of life (Davis M. E. 2016).

Various chemotherapy regimens have been used concurrently with adjuvant radiation in a continuous effort to increase the duration of survival. Significant improvements in survival were not evident until the introduction of Temozolomide (TMZ), an alkylating drug, first in recurrent glioblastoma and then in newly diagnosed patients. Stupp et al., (2002) administered TMZ simultaneously with adjuvant radiation, followed by sequential treatment. They were able to achieve a median survival of 16 months with combination therapy in this early phase II investigation. The combination treatment was shown to have a 27.2% 2-year survival rate when compared to adjuvant radiation in a later randomised study (Stupp, R. et al. 2009). This is still the gold standard therapy for glioblastoma patients under the age of 65 (Gzell, C. et al. 2017).

Another glioblastoma treatment option is hyperthermia, where the temperature of the tumour tissue is increased to 41- 46 °C. This temperature range results in physiological changes to tumour cells potentially leading to apoptosis due to alterations in signal transduction pathways and protein misfolding. The effectiveness of hyperthermia treatment is strongly influenced by the temperature of the targeted tumour location, the characteristics of cancer cells and the duration of exposure. Some methods used to induce hyperthermia use tubes containing boiling water, microwaves, and ultrasounds. However, this approach has several disadvantages such as unintentional

heating of healthy tissue (as a result of heat dispersion through the blood), and inadequate heat diffusion to the target locations (Paolillo, M. et al. 2008).

Glioblastoma tumours that respond to first-line treatment almost always return. There are no effective standard treatments to successfully cure recurrent GBM. Secondary therapy is dependent on the size and location of the tumour, prior therapies, age, and time after the original diagnosis. Surgical resection, reirradiation, temozolomide rechallenge, and tyrosine kinase inhibitors are all options for treatment. Even with these therapies, the median overall survival time with a recurrence is only 6.2 months (Shergalis, A. et al. 2018).

## **1.6 Immunotherapy**

Immunotherapeutic strategies can be classified into different categories: immunomodulatory strategies that target checkpoints, active immunotherapy such as gene therapy or vaccines, and adoptive strategies such as those that use chimeric antigen receptor (CAR) T cells (Kamran, N. et al. 2016).

Targeting immunological checkpoints, which inhibit the immune system from developing a powerful response against the tumour, is a primary focus in cancer treatment (Wilky, B. A. (2019)). On their surfaces, cancer cells are known to express ligands for inhibitory receptors. Inhibitory receptors are recruited to suppress an immune response when they encounter an immune cell (e.g., NK cell or CD8 T cell). The immune systems inhibitory mechanism is operational among malignancies which was proven by targeting CTLA4 to release immune system suppression. Ipilimumab is a monoclonal antibody that has been authorised by the FDA. This antibody targets the CTLA4 receptor and inhibits its interaction with CD80/86, releasing inhibitory signals and enabling cytotoxic T cells to operate as effectors. CTLA4 inhibition was also effective when paired with immune-stimulatory therapies such as radiation or gene virus therapy. CTLA4 blockade will be insufficient alone to promote an enhanced immune response as it is only present on the surface of T cells after stimulation, and glioblastoma is known to be an immunologically suppressed tumour. Therefore, blocking an additional immunosuppressive receptor that is independent of T cell activation should result in a more effective anti-tumour action (Sanders, S. et al. 2020).

The inhibitory receptor PD-1 (programmed cell death 1) is produced by activated T, B, natural killer cells and dendritic cells, as well as activated monocytes and tumour-infiltrating macrophages. It generally protects the host from autoimmunity. PD-1 also affects T-lymphocyte activity in the peripheral tissues, regulating immunity at many stages of the immune response. The PD-1 ligand (PD-L1) is increased on cancer cells in the cancer microenvironment, leading to PD-1 recruitment to the immunological synapse, which suppresses antitumor cytotoxic T lymphocytes. According to a TCGA analysis, high levels of mRNA expression of PD-L1 (PD-1 ligand) and CTLA-4 in glioblastomas implies a link between these immune checkpoint proteins and the severity of the tumour. The prognostic relevance of these immunological checkpoints in glioblastoma is currently debated. Berghoff et al. (2015) examined 117 GBM patient samples and discovered no link between PD-L1 and survival. According to Liu et al. (2013), depending on the glioma subtype, the expression levels of PD-L1 regulatory molecules, and most significantly, the cell type that expresses PD-L1 in the tumour microenvironment, PD-L1 can have both a favourable and negative influence on patient survival. However, most recent clinical investigations have shown that PD-1 and/or PD-L1 are immunohistochemically detectable in most glioblastoma patient samples, and that PD-L1 gene expression is highly related to molecular glioblastoma subtypes. Furthermore, Nduom et al (2016). found that PD-L1 is overexpressed in a small subset of glioblastoma patients, with increased PD-L1 expression associated with a poorer prognosis. Antibodies that inhibit either PD-1 or PD-L1 prevent PD-1 from being recruited to the immunological synapse, allowing cytotoxic T cells to attack the tumour again. Antibodies that inhibit either PD-1 or PD-L1 prevent PD-1 from being recruited to the immunological synapse, allowing cytotoxic T cells to attack the tumour again. Antibody-based blockbuster medications that bind to inhibitory receptors PD-1 or CTLA-4 or their ligands are now authorised in nine countries. While they are very beneficial in some patient subgroups, they are ineffective in others, leaving a significant unmet medical need for more effective cancer treatments. (Duan, S. et al. 2020).

An extracellular tumour-specific antigen-recognition domain and a T cell activation domain are present in genetically engineered T cells that express CARs. CAR T cells have the benefit of being able to detect antigens and activate cell lysis without the need for substantial MHC I presentation. To trigger the anticancer immune response,

autologous or allogeneic T cells are generated in the lab and then adoptively delivered into the patient. In brain tumours, CAR T cells can be injected intravenously, intracranially, or directly into the tumour. Due to glioblastoma heterogeneity, tumour antigen loss during tumour progression, activation of compensatory adoptive resistance mechanisms, and upregulation of immunosuppressive factors and cells (e.g., PD-L1, and Tregs) in the TME that are triggered after CAR T cell application, CAR T cells must be combined with other therapies or with CAR T cells targeting multiple different antigens. Preclinical investigations have shown that trivalent CART T cells targeting human epidermal growth factor receptor 2 (HER2) are more effective than bivalent or monovalent CART T cells. In glioblastoma, CAR T cells targeting tumour-initiating cells via the surface receptor CD133 (tumour initiating surface biomarker) have recently been developed (Majc, B. et al. 2021).

Another strategy used to produce tumour-specific immune response is vaccine therapy. Vaccinations are used to prepare the immune system for infections by exposing the body to immunogenic but inactive microbial antigens, which creates immunological memory despite the absence of previous infection (Wilcox, J. et al. 2018). It includes priming antigen-presenting cells (APCs) are primed with tumour-derived antigens in order to speed tumour cell elimination. Dendritic cells (DCs) are the strongest and most effective in activating T-cells activators, making them appealing targets for therapeutic anticancer methods. DCs are active in both the innate and adaptive immune systems and display high levels of cell surface markers MHC class I/class II and CD86. DCs process antigens more slowly than other APCs, resulting in a longer and more sustained T-cell response. As a vaccination treatment, autologous DCs exposed to glioblastoma-associated antigens are injected back into patients to pick up and digest the antigens as peptides on their cell surface in the setting of MHCs. Dendritic cells can also increase natural killer (NK) and natural killer T (NKT) cell activity, both of which can have a potent antitumor impact (Huang, B. et al. 2017).

### **1.7 Siglecs and sialic acid**

In 1998, the term “Siglec” was developed to identify a subgroup of the Ig gene family that bound sialic acid. Siglecs are type I (single pass) transmembrane surface



proteins, which are also known as Ig-like lectins (Varki, A. et al. 2006). Siglecs have an N-terminal variable set (V-set) domain for the purpose of binding sialic acid-containing glycan ligands, and a conserved arginine residue for carbohydrate binding activity within the V-set domain. Most Siglecs have one or more cytoplasmic tyrosine residues placed within certain signalling domain topologies, particularly those implicated in inhibiting responses (for example, immunoreceptor tyrosine-based inhibitory motifs – ITIMs). In relation to species homology, Siglec-1, Siglec-2 (CD22), Siglec-3 (CD33), Siglec-4 and Siglec 15 are highly conserved and thus have the same names in all mammals. In contrast, the remaining CD33-related members, grouped together on chromosome 19q13.3-13.4, are more structurally and evolutionarily diverse (Von Gunten, S. et al. 2008).

Sialic acids are found on the outer end of glycan chains on the cell surface, and they contain nine-carbon sugars. They play important roles as recognition components in host pathogen interactions and cell – cell communication (Hayakawa, T. et al. 2017). They can, however, occasionally be joined together to form short or long homopolymers called polysialic acid. Polysialic acid is made up of  $\alpha$ 2–8–linked Neu5Ac units and is present on several proteins in the brain. This structure has a role in the development, function and morphogenesis of numerous neural systems. Polysialic acid has been found on a few immune cells, including dendritic cells and certain phases of T cell development (Varki, A., & Gagneux, P. 2012). Polysialic acid can reach lengths of 100+ residues and is a linear homopolymers of sialic acid. Shorter chains are known as oligosialic acid, and are usually 2-3 residues long. Poly sialic acid is a major structural feature of a highly selective collection of acceptor proteins, the most well-studied of which being the neural cell adhesion molecule (NCAM). Beginning early in vertebrate brain development, long poly sialic chains are attached to NCAM at the termini of two specific N-glycans. The hydration shell of PolySia increases the hydrodynamic volume of its protein carrier and disrupts the NCAM's cell–cell adhesion function. Polysia converts a sticky protein into one that repels. A high level of polySia during brain development ensures that neural precursors can progress to their final anatomical destinations. When a cell reaches its destination, polySia is downregulated and strong adhesion results in keeping the cells together (Varki, A. et al. 2017).

In 2002, Siglec-11 was reported as a primate-specific gene with a human specific expression pattern. Siglec-11 was shown to be broadly expressed on tissue macrophages in humans, including microglia in the brain. Figure 4 shows the expression of Siglec-11 in a normal sample of the body compared to that of a tumour one. Siglec-11 features ITIM motifs in its cytoplasmic tail, like other inhibitory Siglecs (Linnartz-Gerlach, B. et al. 2014). The cytoplasmic domain contains numerous immunoreceptor tyrosine-based inhibitory motifs (ITIMs), which interact with Src homology domain 2-containing phosphatase-1 (SHP-1) and SHP-2 following tyrosine phosphorylation. SHP-1 has a role in microglia anti-inflammatory signalling. Siglec-11, on the other hand, has various unique characteristics that set it apart from other CD33-related Siglecs. First, it binds to 2,8-linked sialic acids (Linnartz-Gerlach, B. et al. 2014), the ligand molecule changed by 2,8-linked sialic acids and recognised by Siglec-11 remains unknown. As a result, polysialic acid (PSA), commonly found linked to glycoproteins in the CNS, might be a potential ligand for Siglec-11. Second, Siglec-11 expression was observed on diverse tissue macrophages, including brain microglia (Wang, Y. et al. 2010).

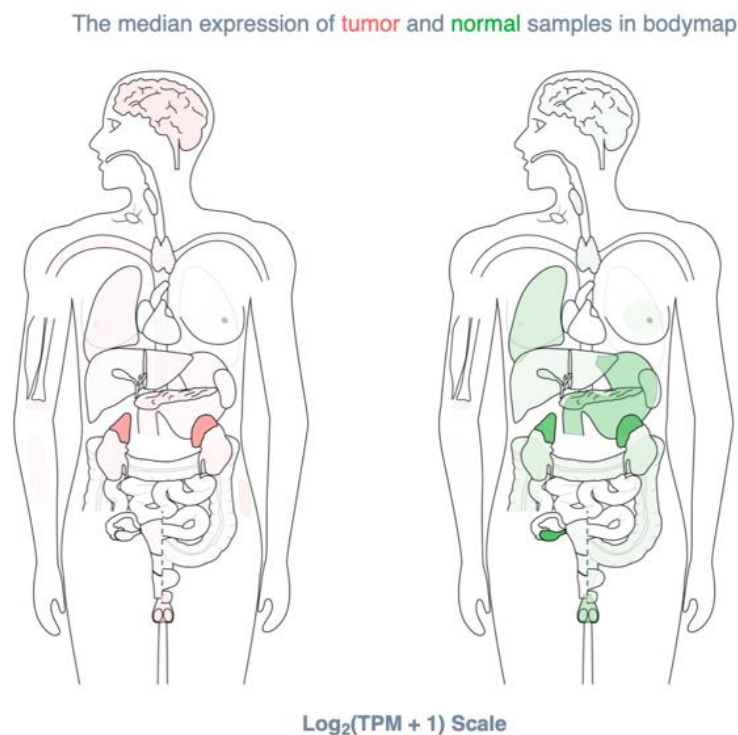


**Figure 4.** A comparison between a normal human body that expresses Siglec-11 compared to a tumour one. Image from Gepia2.

In 2001, the human genomic DNA sequence corresponding to Siglec-15's N-terminal immunoglobulin-like domain was initially discovered. Siglec-15 features an extracellular domain with two immunoglobulin-like domains, a transmembrane domain containing a lysine residue required for interaction with the adaptor protein DAP12, and a cytoplasmic tail. DAP12 features a small extracellular domain (less than 20 amino acids), a transmembrane domain with an aspartic acid residue, and a cytoplasmic tail with a sequence pattern called immunoreceptor tyrosine-based activation motif (ITAM). As with many other receptors that bind with DAP12, the interaction between Siglec-15 and DAP12 is based on an ionic bond at the transmembrane domains (Angata, T. 2020). Figure 5 shows the expression of Siglec-15 in a normal sample of the body in comparison to a tumorigenic patient.

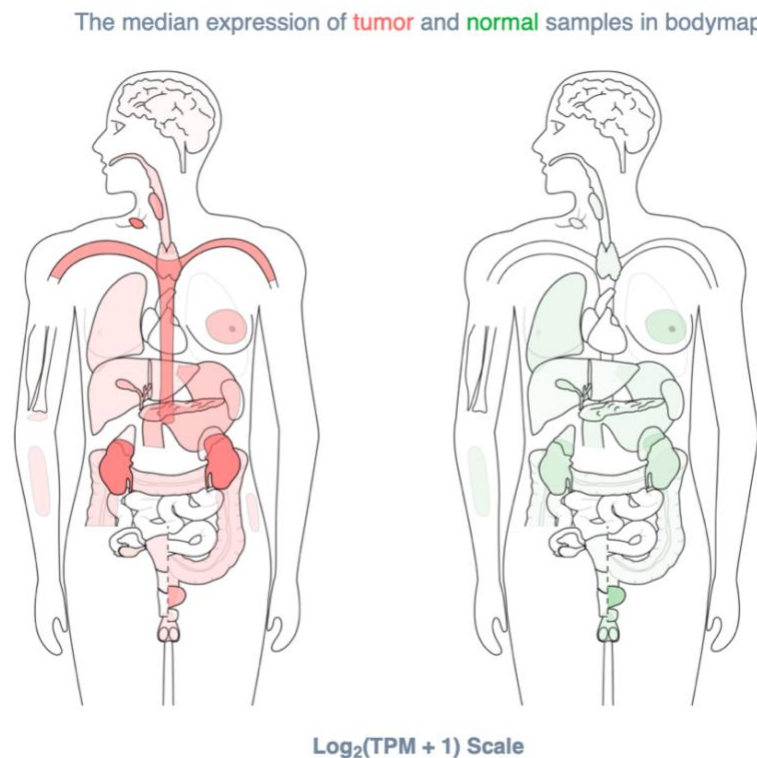


**Figure 5.** A comparison between a normal human body that expresses Siglec-15 compared to a tumour one. Image from Gepia2.

### 1.8 Potential treatments

More than 80% of glioblastomas have p53 and Retinoblastoma/E2F tumour suppressor pathway disruption. On DNA damage, *TP53* encodes the tumour suppressor protein p53, which induces cell-cycle arrest and promotes apoptosis. *TP53*

mutation or deletion promotes glioma cell proliferation and clonal expansion, as well as DNA repair impairment, promoting genomic instability. Initial p53-targeting therapies attempted to reactivate these pathways by gene therapy and pharmacological techniques, but failed to be clinically effective (Touat, M. et al. 2017).

Angiogenesis, blood vessel formation, is the rate-determining mechanism for solid tumour development and is also a primary characteristics of tumour tissues (Huang, S. et al. 2013). Glioblastoma has high angiogenesis rates. Many stimulating and inhibitory factors are involved in tumour angiogenesis. As a result, various potential techniques for glioblastoma treatment exist, such as downregulating the expression of stimulating factors. For example, the ErbB family of receptor tyrosine kinases (RTKs) include the epidermal growth factor receptor (EGFR). EGF ligand binding activates the RTK/RAS pathway, resulting in cellular proliferation, enhanced local tissue invasion, and resistance to apoptosis (Padfield, E. et al. 2015). EGFR is overexpressed in ~50% of glioblastoma patients. Nearly 50% of GBMs have gain-of-function EGFRvIII mutations (EGFR variant III). EGFRvIII is the result of a genomic deletion of exons 2–7, which encode the receptor's ligand-binding domain, resulting in constitutively active oncogenic receptor tyrosine kinases. Furthermore, EGFRvIII cell signalling can result in EGFR inhibitor resistance and cause poor long-term survival. Currently an anti-EGFRvIII vaccination (rindopepimut) is in development and is due to start clinical trials (Xu, Y. et al. 2015).

Research has shown that miRNAs play critical roles in glioblastoma and other tumours. MicroRNAs (miRNAs) are small non-coding RNA molecules that play an important role in the course of several different malignancies and are being proposed as potential anti-cancer therapeutic targets. Despite the potential of miRNAs, there are complications when using them as cancer treatments. MiRNAs have unstable properties that may affect direct cell membrane penetration. These features include negative charge and hydrophilic properties (Hong, S. et al. 2021). A section of the microRNA known as a 'seed' attaches to a complementary sequence in the target mRNA to guide the suppression of an mRNA molecule. Canonical sites are mRNA regions that contain the precise sequence of partner bases for the microRNA seed bases. Some canonical sites are more successful than others at mRNA control. There are also non-canonical sites, where the pairing of the microRNA seed and mRNA does

not perfectly match. This can influence mRNA usage and degradation (Agarwal, V. et al. 2015).

## **1.9 Hypothesis**

It has been hypothesised that Siglec-11 and Siglec-15 can be used as therapeutic targets in glioblastoma. Both Siglec-11 and Siglec-15 generate immune inhibitory signals upon binding with their ligand. Therefore, miRNAs could be used to regulate the gene expression of both Siglecs and prevent the binding of the protein receptor to its sialic acid ligand.

### **1.9.1 Aims**

The aim of this research is to understand the role of miRNAs in regulating Siglec -11 and Siglec-15 and its overall effect on glioblastoma. The main objective is to determine which miRNAs may regulate the expression of Siglec-11 and Siglec-15 in microglia and glioblastoma.

### **1.9.2 Objectives**

- Initially, bioinformatic analysis for the shortlisting of the miRNAs that may regulate the expression of Siglec-11 and Siglec-15 in microglia and glioblastomas.
- Then, perform real time polymerase chain reaction (RT-qPCR) to validate the expression of the miRNAs.
- Identify different gene targets using different bioinformatic tools and perform RT-qPCR and western blot to validate their expression.

## 2. Methods

### 2.1 Bioinformatics

The bioinformatic analysis was completed using several online tools. Targetscan ([https://www.targetscan.org/vert\\_72/](https://www.targetscan.org/vert_72/)) and miRSystem (<http://mirsystem.cgm.ntu.edu.tw>) were used to identify which miRNAs are involved in the regulation of both Siglec-11 and Siglec-15. Gene Expression Profiling Interactive Analysis -GEPIA2 (<http://gepia2.cancer-pku.cn/#index>) was used to identify the expression and survival of Siglec-11 and Siglec-15 between cancer patients and healthy individuals. DIANA (<https://diana.e-ce.uth.gr/tools>) and miRwalk (<http://mirwalk.umm.uni-heidelberg.de>) were both used alongside Targetscan and miRSystem to identify different miRNAs that play a role in tumours. Once results were obtained, VENNY 2.0 (<https://bioinfoq.cnb.csic.es/tools/venny/>) was used to create a diagram that distinguishes the similar miRNAs that are present in the list created using the bioinformatic tools.

### 2.2 Cell culture

Human glioblastoma cell lines U87MG and A172 were obtained from the American type culture collection – ATCC (Virginia, USA). A172 cell line was cultured at 37°C and 5% CO<sub>2</sub> in Dulbecco's modified Eagle's medium – DMEM (Gibco, Bleiswijk, Netherlands), U87MG was cultured at 37°C and 5% CO<sub>2</sub> in Eagle's MEM (Gibco, Bleiswijk, Netherlands). Complete media was supplemented with 10% fetal bovine serum – FBS (Fisher scientific; UK) and 1% Penicillin, Streptomycin (Gibco, Bleiswijk, Netherlands) for both. Both cell lines were cultured for experimental use upon reaching confluency of 80% and above.

### 2.3 MiRNA isolation

MiRNA isolation was performed to homogenize a pellet of A172 cells from a T75 flask with at least 85% confluency, 0.4 ml (400 ul) of Trizol (Ambion Life Technology, Auckland, New Zealand) was added to a 15 ml falcon tube that contains the cells. The Trizol was added using a 5 ml syringe. Subsequently, the cells were left to incubate in Trizol for 5 mins at room temperature to allow the complete dissociation of the nucleoproteins complex. After incubation, the Trizol cell homogenate was transferred

to a 1.5 ml RNase free Eppendorf tube. Then, 0.08 ml (80  $\mu$ l) of chloroform was added to this Eppendorf to allow the cell homogenate to separate into different layers. The Eppendorf was vortexed at medium speed to ensure the content was well mixed and then left to incubate at room temperature for 2-3 mins. After incubation, the Eppendorf was centrifuged (Biofuge Fresco, Germany) for 15 mins at 12,000xg (11.2 rpm) at 4°C. The centrifugation resulted in the sample separating into different layers: a lower red phenol-chloroform layer containing proteins, an interphase layer containing DNA and a colourless upper aqueous layer containing RNA. The colourless upper aqueous layer containing the RNA was transferred into a new RNase free 1.5 ml Eppendorf tube containing 0.2 ml (200  $\mu$ l) of isopropanol. The sample was incubated for 10 mins at 4°C. After incubation, the sample was centrifuged at 12,000xg (11.2 rpm) at 4°C to allow the RNA precipitate to form a white gel-like pellet at the bottom of the Eppendorf tube. After centrifugation, the isopropanol was discarded using a micro-pipettor. Two wash steps were performed using the addition of 0.4 ml (400  $\mu$ l) 75% ethanol to resuspend the pellet and then vortexing the sample to ensure complete mixing. The sample was centrifuged for 5 mins at 7500xg (8.8 rpm) at 4°C for each step. After the two wash steps, the ethanol was discarded from the Eppendorf and the tube was left open to allow the RNA pellet to air dry for 5-10 mins. After the air-dry step, 0.02 ml (20  $\mu$ l) of RNase-free water was added to the tube and the sample was incubated on a heat block that was set at 58°C for 10-15 mins. To measure the quantity and quality of this sample, a Nanodrop (Nanodrop ND1000 Spectrophotometer, Virginia, USA) was used. Finally, the sample was made up to 0.1 ml (100  $\mu$ l) kept in the freezer at -20°C.

## **2.4 Organic Extraction**

After assessing the quality and quantity of the sample using the Nanodrop (Nanodrop ND1000 Spectrophotometer, Virginia, USA), the sample was purified and extracted. In brief, 10  $\mu$ l of homogenate additive were added to the sample. The Eppendorf tube was then vortexed and left to incubate on ice for 10 mins. Next, a volume of Acid – Phenol: Chloroform (Ambion, Texas, USA) equal to the volume of the lysate was added to the Eppendorf tube (lysate volume was 100  $\mu$ l so added volume was also 100  $\mu$ l). It was ensured that the Acid – Phenol: Chloroform was withdrawn from the bottom phase of the bottle as the upper phase contained the aqueous buffer. The

Eppendorf tube containing the sample was vortexed and then centrifuged for 5 mins at 10,000 xg at room temperature. This resulted in two layers being formed: an organic phase layer and an aqueous layer. The aqueous layer formed at the top of the Eppendorf tube. It was removed and added to a new RNase free Eppendorf. The volume removed was noted down for reference. A volume of 1.25 (x 1.25) of 100 % ethanol at room temperature was then added to the new Eppendorf tube containing the aqueous layer. From the mirVana isolation kit (ThermoFisher, Vilnius, Lithuania), a filter cartridge was placed onto a collection tube. The lysate was pipetted directly onto the middle of the filter cartridge, ensuring that it didn't touch the sides. For the lysate to flow through the filter cartridge, the collection tube was centrifuged for 15-30 secs at 10,000xg at room temperature. The flowthrough in the collection tube was discarded, then the tube was centrifuged again for 15 secs at 10,000xg at room temperature to ensure that everything was removed from the filter cartridge. For the washing steps, the same collection tube was used. The first wash step involved 700 µl of solution 1 pipetted directly onto the centre of the filter cartridge, which was included in the miRVana isolation kit. The collection tube was centrifuged for 15-30 secs at 10,000xg at room temperature to allow the wash solution could flowthrough. Next, the flow through in the tube was discarded and the tube was centrifuged for 15 secs at 10,000xg at room temperature to ensure that any remaining wash solution 1 can flow through. The second wash step included wash solution 2/3, which was supplied in the miRVana isolation kit. From wash solution 2/3, 700 µl was pipetted onto the centre of the filter cartridge. The collection tube was centrifuged for 15-30 secs at 10,000xg at room temperature. Under the same conditions, the tube was centrifuged again for 1 min in order to allow the wash solution to flow through. After centrifugation, the filter cartridge was removed and transferred to a new collection tube. Using pre-heated eluent buffer, 75 µl was pipetted to the centre of the filter cartridge. In order to recover the RNA contents from the filter, the tube was centrifuged at maximum speed for 30 secs. Once this was completed, the eluent containing RNA content was collected then quantitative and qualitative analysis was performed using Nanodrop (Nanodrop ND1000 Spectrophotometer, Virginia, USA).



## 2.5 cDNA synthesis

The Reverse Transcription (RT) Reaction Mix was prepared as the initial stage in cDNA synthesis. Then, the component of the reverse transcription kit was all thawed on ice. The following RT primers from Applied Biosystems (ThermoFisher, Pleasanton, CA) were thawed on ice: hsa-miR-138-5p, hsa-miR-153 and hsa-miR-107. The RT reaction mix was prepared using the volumes listed in the table below:

**Table 1.** RT reaction mix volumes.

<b>Component</b>	<b>Volume (1 reaction)</b>	<b>Volume (3 reactions)</b>
100mM of dNTPs	0.15 $\mu$ l	0.45 $\mu$ l
MultiScribe <sup>TM</sup> Reverse Transcriptase, 50 U/ $\mu$ l	1.00 $\mu$ l	3 $\mu$ l
10X Reverse Transcription Buffer	1.50 $\mu$ l	4.50 $\mu$ l
RNAse Inhibitor, 20 U/ $\mu$ l	0.19 $\mu$ l	0.57 $\mu$ l
Nuclease-free Water	4.16 $\mu$ l	12.48 $\mu$ l
Total RT Reaction Mix volume	7 $\mu$ l	21 $\mu$ l

For each miRNA primer, four RT reaction mixes were prepared. The volume of the RT reaction mixes was prepared for 3 reactions: one volume for the miRNA, one volume as a control and one volume as an extra to allow for any pipetting errors.

The eluent RNA sample had to be diluted for cDNA synthesis, such that only 1-10 ng of RNA was used in the procedure. The original sample was diluted by applying the  $C_iV_i=C_fV_f$  equation. Once obtained, the RNA sample volume was moved to a new RNase-free tube, and the volume was increased to 20  $\mu$ l by adding nuclease-free water.

To prepare the RT reaction mix, 7  $\mu$ l of the RT mix were added to PCR tubes along with 5  $\mu$ l of the 1-10 ng sample of RNA. The PCR tube was vortexed and then centrifuged briefly to ensure the contents were thoroughly mixed. Following this, 3  $\mu$ l of 5 x RT primer for each miRNA was added to each allocated PCR reaction tube. Each reaction tube had a final volume of 20  $\mu$ l. The tubes were centrifuged briefly

before being transferred to the Thermal cycler (Eppendorf, Mastercycler nexus gradient, Stevenage, UK). Once placed in the Thermal cycler, reverse transcription was performed following the conditions mentioned in the Table below:

**Table 2.** Conditions for RT reaction.

<b>Step</b>	<b>Temperature</b>	<b>Time</b>
Reverse Transcription	16°C	30 min
	42°C	30 min
Stop Reaction	85°C	5 min
Hold	4°C	Hold

### 2.6 Quantitative Real time Polymerase Chain Reaction (RT-qPCR)

The miR primers (20X) for RNU-44, miR-138-5p, miR-153-3p, and miR-107, as well as the cDNA templates, were thawed out on the ice, vortexed, and centrifuged to pellet the tube contents prior to plating the samples on a 96-well PCR plate. The following table was used to prepare the PCR Reaction mix:

**Table 3.** RT-qPCR reaction mix volumes.

<b>Component</b>	<b>Volume per reaction</b>	
	<b>96-well standard (0.2 ml) plate (1 reaction)</b>	<b>96-well standard (0.2 ml) plate (5 reaction)</b>
TaqMan™ Small RNA Assay (20X)	1.00 µl	5.00 µl
PCR Master Mix	10.00 µl	50.00 µl
Nuclease-free Water	7.67 µl	38.35 µl
Total PCR Reaction Mix Volume	18.67 µl	93.35 µl

The PCR mix was kept on ice along with the rest of the reaction components. Per cDNA sample, three 1.5 ml RNase free Eppendorf's were used. One Eppendorf was used for background control, it contained the primer and template but with no master mix. One Eppendorf was used as a negative control, it contained the master mix and primer but no template. Finally, the third tube contained all three: the PCR master mix, template and primer.

On a 96-well plate, 20  $\mu$ l of the reaction mixes for each prepared sample and its associated miRNAs were pipetted in mechanical triplicates. The plate was then vortexed and centrifuged to move the contents of the samples to the bottom of the well. Following this, the RT-qPCR was performed using QuantStudio™ Real-Time PCR (Applied Biosystems, Foster City, California, USA) under the conditions mentioned in the table below:

**Table 4.** Conditions for RT-qPCR reaction.

<b>Step</b>	<b>Temperature</b>	<b>Time</b>	<b>Cycles</b>
Enzyme activation	95°C	10 min	1
Denature	95°C	15 sec	40
Anneal/Extend	60°C	60 sec	

## 2.7 RT-qPCR with genes

Prepare sample as instructed in the 2.3 MiRNA Isolation method section. Following this, prepare the sample by adding 89  $\mu$ l of RNase free water, 10  $\mu$ l of RDD buffer and 2.5  $\mu$ l DNase 1 stock solution. The final volume of the sample should be 100  $\mu$ l. Once the sample is ready, the next step is to prepare the RT master mix on ice using the following table:

**Table 5.** RT Master Mix without RNase inhibitor components and volumes

<b>Component</b>	<b>Volume (1 reaction) without RNase inhibitor</b>	<b>Volume (3 reactions) without RNase inhibitor</b>
10X RT Buffer	2.0 $\mu$ l	6.0 $\mu$ l
25X dNTP Mix (100mM)	0.8 $\mu$ l	2.4 $\mu$ l
10X RT Random Primers	2.0 $\mu$ l	6.0 $\mu$ l
MultiScribe™ Reverse Transcriptase	1.0 $\mu$ l	3.0 $\mu$ l
RNase Inhibitor	-	-
Nuclease-free H <sub>2</sub> O	4.2 $\mu$ l	12.6 $\mu$ l
Total per reaction	10.0 $\mu$ l	30.0 $\mu$ l

Once the RT Master Mix was complete, pipette 30  $\mu$ l was pipetted and mixed in a tube containing 30  $\mu$ l of the sample. This was mixed gently and measured using Nanodrop (Nanodrop ND1000 Spectrophotometer, Virginia, USA). After measurement, cDNA

treatment using the Thermal cycler was performed using the conditions in Table 6 (Eppendorf, Mastercycler nexus gradient, Stevenage, UK).

**Table 6.** Conditions for Fast Advanced Master Mix

Step	Temperature	Time	Cycles
Enzyme activation	95°C	20 sec	1
Denature	95°C	1 sec	40
Anneal/Extend	60°C	20 sec	

The components for the PCR Reaction Mix and the two genes: Siglec-15 and GAPDH, were thawed out on ice, vortexed, and centrifuged to bring the contents of the tubes to the bottom prior to plating the samples on a 96-well PCR plate. The PCR Reaction Mix was prepared according to Table 7:

**Table 7.** RT-qPCR reaction mix volumes.

Component	Volume per reaction	
	96-well standard (0.2 ml) plate (1 reaction)	96-well standard (0.2 ml) plate (4 reaction)
TaqMan™ Small RNA Assay (20X)	1.00 µl	4.00 µl
PCR Master Mix	10.00 µl	40.00 µl
Nuclease-free Water	7.67 µl	30.68 µl
Total PCR Reaction Mix Volume	18.67 µl	74.68 µl

Once completed, the PCR Reaction Mix was vortexed briefly and transferred into an optical reaction plate. In this case, add 18.67 of the PCR Reaction Mix into a 96-well standard (0.2 mL) plate and 1.33 µl of the cDNA template. For no template control wells (NTC), add 18.67 µl of Master Mix and 1.33 µl of nuclease free water. The plate was then vortexed and centrifuged to move the contents of the samples to the bottom of the well. Subsequently the RT-qPCR was performed using QuantStudio™ Real-Time PCR (Applied Biosystems, Foster City, California, USA) under the conditions mentioned in Table 4.

## 2.8 Western blots

To prepare samples for Western Blot, the protein concentration (From BCA Assay) was diluted with 15 µl diluent (RIPA buffer) and added 5 ul of Lammeli buffer to result in a 30-µg solution. Once the buffers are added, heat at 95 °C for 5 mins using the heat block.

### Western blot preparation:

- **Preparation of gels**
- **Resolving gel:**

30% Acrylamide stock (3.33 ml), 1.5 M Tris-HCL (2.50 ml), distilled water (4.015 ml), 10% SDS (100 ul), APS (50 ul) and TEMED (5 ul).

Mix and wait for 45-60 mins to solidify. After adding resolving gel to set, add 100-200 ul of water on top with a dropper to even out the gel, then remove any excess water with filter paper once the gel is set.

- **Stacking gel:**

30% Acrylamide stock (1.33 ml), 0.5 M Tris-HCL (1.25 ml), distilled water (2.34 ml), 10% SDS (50 ul), APS (25 ul) and TEMED (5 ul).

Add stacking gel on top of the resolving gel. Wait to solidify for 45-60 mins.

- **Preparation of buffers**

Recipe obtained from Bio-Rad 'A guide to polyacrylamide gel electrophoresis and detection'.

**10x Running buffer (pH 8.3):** Tris base (30.30 g), Glycine (144.10 g) and SDS (10 g). Add distilled water until the final volume is 1 L. For 1x running buffer, dilute 100 ml of 10x running buffer to 900 ml of distilled water.

**10x Transfer buffer (pH 8.1-8.5):** Tris base (30.30 g), Glycine (144.10 g) and distilled water (make up final volume to 1 L). For 1x transfer buffer, dilute 100 ml of 10x Transfer buffer to 400 ml of distilled water and 200 ml of 100% methanol (adjust volume to 1 L).

**4x Lammeli buffer:** 2.5 M Tris-HCL (30.3 g in 100 ml diH<sub>2</sub>O), 10% SDS (2 g in 20 ml diH<sub>2</sub>O) and 1% Bromophenol blue (100 mg in 10 ml diH<sub>2</sub>O).

**10x TBS buffer (pH 7.6):** Tris base (12 g), NaCl (44 g). Adjust volume to 500 ml using distilled water. For 1x TBS buffer, dilute 100 ml of 10x stock with 900 ml of distilled water and 1 ml Tween-20 detergent.

After preparing the sample, 2 ul of pre-stained ladder and 20 ul of sample were loaded. Running buffer was added to the cassette. Following this step, the gel was run at 100V for 100 mins. The nitrocellulose membrane was prepared according to the gel size. The gel, the membrane, pads and filters were equilibrated in transfer buffer for 5 mins. The transfer sandwich was assembled in the following order: black frame (negative electrode), foam, filter paper, SDS gel, membrane, filter paper, foam and finally, the red frame (positive electrode). The gel was run at 100V for 60 mins, ensure it is placed in an ice tray and surrounded by ice in order to prevent overheating the buffer. After the transfer, the membrane was blocked in 3% milk/TBS buffer, put in boxes and then placed on a rocker for 1 hour. After the time is done, fresh 3% milk/TBS buffer with primary antibody was prepared using a 1 in 1000 dilution and covered the membrane. It was left on a rocker overnight at 4°C. After primary antibody overnight incubation, it was washed with 1x TBST buffer 3 times, 5 mins for each wash step. Membranes were transferred into black boxes and secondary antibody dilution in 1x TBST by adding 2 ul of antibody into 2 ul of TBST was prepared. The mixture of antibody and TBST was added to the membrane and incubate on rocker for 1 hour. Post the incubation, gels were washed with TBST 3 times, 5 mins for each wash step. Chemiluminescent substrate was added directly onto the membrane (0.06 ml per cm<sup>2</sup>) left for 1 min, then remove by pressing down firmly to ensure that there are no air bubbles remaining. Gel was visualises using the western blot imagine and analysis machine.

## 3. Results

### 3.1 Bioinformatic analysis results

**Table 8. Identification of target miRNA for Siglec-11 and Siglec-15 through bioinformatics analysis:** Different miRNAs were selected from multiple bioinformatic analysis including Target Scan Human and miRSystem, then further analysed using previous and current literature research. Some of the miRNAs including hsa-miR-138-5p were found to be highly downregulated in GBM.

Genes	Name of miRNA	Tool used	Known about GBM	Known about Immunoregulation/Microglia activation	Any other cancer	Upregulated/downregulated in cancer	References
Siglec- 11	Hsa-miR-1266-3p	Target Scan Human	NA	NA	A miRNA that promotes breast and pancreatic cancer by targeting several negative regulators of the STAT3 and NF-kB signalling pathways, hence encouraging cell survival and aiding in chemotherapy resistance.	NA	Micolucci, L. et al. 2016.
Siglec- 11	Hsa-miR-138-5p	Target Scan Human	MiR-138-5p has been proposed to operate as a tumour suppressor gene in GBM by targeting CCND3, resulting in cell cycle arrest and suppression of	NA	MicroRNA (miR) 138 5p has been identified as a tumour suppressor in a variety of human cancers, including non-small cell lung carcinoma (NSCLC) and chronic myeloid leukaemia (CLL).	MiR-138-5p expression was shown to be highly downregulated in GBM tissues and cell lines.	Henggang Wu, et al. 2020  Margret Yeh, et al. 2019



			tumour cell survival and colony formation, implying that miR-138-5p might be a viable diagnostic and/or therapeutic target for GBM.				
Siglec- 11	Hsa-miR-133a-5p	Target Scan Human	MiR-133a-5p is downregulated in glioma cells by promoter hypermethylation, and its forced expression reduces glioma cell growth and causes G1 phase arrest via PGC-1 targeting.	NA	MiR-133a-5p expression was considerably reduced in prostate cancer, and low miR-133a-5p expression was associated with a worse chance of survival.	Downregulated.	Liu, L. et al. 2020.  Zheng, L. et al. 2020.
Siglec- 11	Hsa-miR-6131	Target Scan Human	NA	NA	The function of miR-6131 is unclear, and it is conceivable that	NA	Fujita, K. et al. 2015.

					miR-6131 plays no role in cancer progression suppression.		
Siglec- 11	Hsa-miR-505-3p.2	Target Scan Human	NA	NA	505-3p – was shown to be highly elevated in synovial sarcoma patients as compared to leiomyosarcoma, MPNST and liposarcoma patients by qRT-PCR.		Fricke, A. et al. 2015.
Siglec-15	Hsa-miR-375	Target Scan Human	In patients with gliomas, downregulation provides poor overall survival.	Found to be implicated in cancer related processes such as cell cycle regulation by E2F3.	It has been reported to be downregulated in oesophageal carcinoma and gastric cancer. However, it is upregulated in primary prostate carcinoma.	Downregulated -	Toraih, E. et al. 2017.
Siglec-15	Hsa-miR-1202	Target Scan Human	Overexpression inhibited proliferation and induced ERS and apoptosis of glioma cells. It targets Rab1A.	NA	MiR-1202 has been suggested as a molecular tumour marker in different tumours including hepatocellular carcinoma.	Downregulated.	Quan, Y. et al. 2017

Siglec-15	Hsa-miR-215-5p	Target Scan Human	miR-215-5p is upregulated in gliomas, especially in high grade ones.	NA	MiR-215-5p targets EGFR ligand in colorectal cancer and can act as a tumour suppressor	Upregulated – used to downregulate PCDH9 (a protein coding gene)	Wang, C. et al. 2016.  Vychytilova-Faltejskova, P. et al. 2017
Siglec- 11	Hsa-miR-133a-3p	miRSystem	NA	NA	MiR-133a-3p is a common tumour-associated miRNA that serves as a tumour suppressor to inhibit cancer formation by regulating target genes in breast cancer, gastric cancer, pancreatic cancer, and glioma.		Li, J. et al. 2020.
Siglec- 11	Hsa-miR-133b	miRSystem	MiR-133b inhibited GBM cell migration and invasion. MiR-133b may inhibit GBM migration and invasion by directly targeting MMP14 (a direct target gene),	NA	MiR-133b expression has been found to be abnormal in cancers such as cervical carcinoma, lung cancer, renal cell carcinoma, colon cancer, osteosarcoma, and prostate cancer. MiR-133b has been proposed to act as	MiR-133b was commonly shown to be downregulated in GBM tumour tissues.	Chang, L. et al. 2015.

			indicating its potential as a new drug for GBM invasion therapy.		a tumour suppressor in some forms of cancer by directly targeting certain oncogenes.		
Siglec- 11	Hsa-miR-485-5p	miRSystem	The expression of miRNA-485-5p was decreased in glioma tissues and cell lines. Furthermore, overexpression of miRNA-485-5p decreased cell proliferation, migration, and invasion in glioma cell lines.	NA	MiR-485-5p expression is considerably lower in gastric cancer tissues compared to normal tissues, making it a new biomarker for overall survival in gastric cancer patients. MiR-485-5p also decreases cell proliferation in hepatocellular carcinoma, and its overexpression in breast cancer cells prevents spontaneous metastasis in vivo. Previous research suggests that miR-485-5p may act as a tumour suppressor, and that its	miRNA-485-5p inhibited glioma tumorigenesis in vitro and in vivo by downregulating TPD52L2 (target gene in glioma cells) expression.	Yu, J. et al. 2017.

					downregulation may lead to glioma tumorigenesis.		
Siglec- 11	Hsa-miR-10a-5p	miRSystem	NA	Involved in the regulation of the tumour microenvironment by glioma.	In solid tumours, it is known to have a tumour suppressive action. MiR-10a-5p suppressed tumour growth in breast cancer and hepatocellular carcinoma.	In late cancer stages, it is found to be under expressed.	Worst, T. et al. 2020.
Siglec- 11	Hsa-miR-10b-5p	miRSystem	Previous research has demonstrated that miR-10b-5p promotes cell proliferation in glioblastoma.	NA	It has been established that it plays an oncogenic role. A meta-analysis of 19 studies involving sporadic tumour types such as colorectal cancer, breast cancer, pancreatic cancer, non-small cell lung carcinoma, and gliomas found a link between miR-10b overexpression and poor overall survival. Previous functional studies in	NA	Ru, Q. et al. 2018.  Nix, J. at al. 2021.

					<p>glioma cell lines have shown that miR-10b has a role in radiation resistance, proliferation, and apoptosis suppression.</p> <p>When comparing NF1-high-grade glioma to NF1-low-grade glioma, the miR-10b-5p microRNA was found to be overexpressed. Adult glioma cell lines had the greatest levels of miR-10b-5p, whereas paediatric low-grade glioma cell lines had the lowest.</p>		
Siglec- 11	Hsa-miR-139-5p	miRSystem	Evidence suggests that miR-139-5p inhibits the development of GBM. In GBM	NA	miR-139-5p is one of the most important miRNAs discovered to play a role in human tumorigenesis. It has been found to	The miRNA array revealed that microRNA-139-5p	<p>Dai, S. et al. 2015.</p> <p>Yue, S. et al. 2015.</p>

			multiforme, for example, miRNA-139-5p works as a tumour suppressor by targeting ELTD1 and regulating the cell cycle. MiR-139-5p inhibits cancer cell migration and invasion in GBM by targeting ZEB1 and ZEB2.		be relevant to numerous tumour types and drastically downregulate them, including breast cancer, and GBM.	was considerably down-regulated in glioblastoma a multiforme (GBM).	
--	--	--	--	--	---	---	--

The different bioinformatic tools that have been used above revealed many miRNAs that are associated with GBM and other cancer types. Hsa-miR-133b was shown to be downregulated in GBM by inhibiting cell migration and invasion. This critical analysis can be used to identify certain miRNAs and study their regulation in GBM to further use them in the development of effective cancer therapeutics.

Another bioinformatic analysis was carried out involving 4 different tools: DIANA, miRSystem, miRWalk and Target Scan. These bioinformatic tools were used to identify the predicted miRNA that regulate gene expression of the query gene (Siglec-11). Once all the data was obtained, it was placed into VENNY 2.0 in order to find any similarities across all 4 tools. The results obtained suggested that the following miRNAs have been found in all the tools mentioned above: hsa-miR-485-5p, hsa-miR-10a-5p, hsa-miR-138-5p, hsa-miR-339-5p, has-miR-410-3p, hsa-miR-532-3p, hsa-miR-650, hsa-miR-657, hsa-miR-665 and hsa-miR-24-3p.

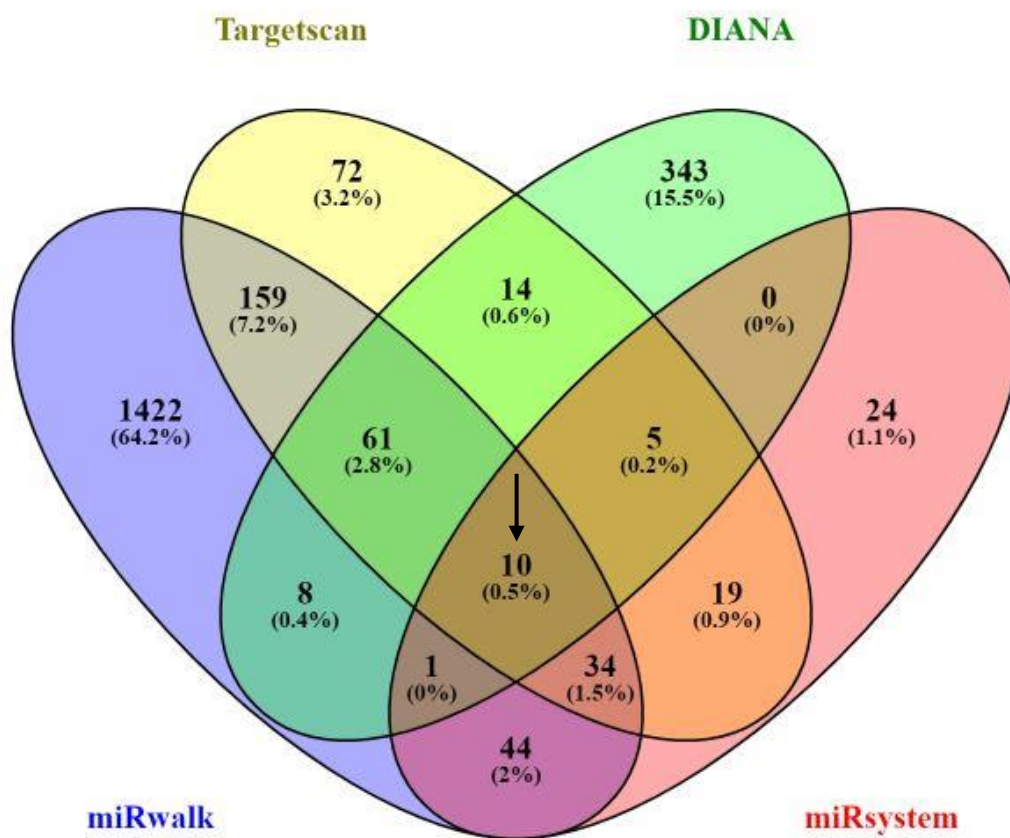


**Figure 6.** Analysis of various bioinformatic tools to show the similarity of miRNA hits found. Image created using VENNY 2.0.



The boxplots for the corresponding Siglecs demonstrated overexpression of Siglec-11 and Siglec-15 in glioblastoma tissue samples (n=163) when compared to normal brain tissue samples (n=207). Figure 7a for Siglec-11 showed a more significant upregulated expression. The overexpression of both Siglec-11 and Siglec-15 was found to have no statistical significance. This might be due to the small sample size of the contrasted groups, for which more individuals are needed to confirm or deny the significance of their expression.

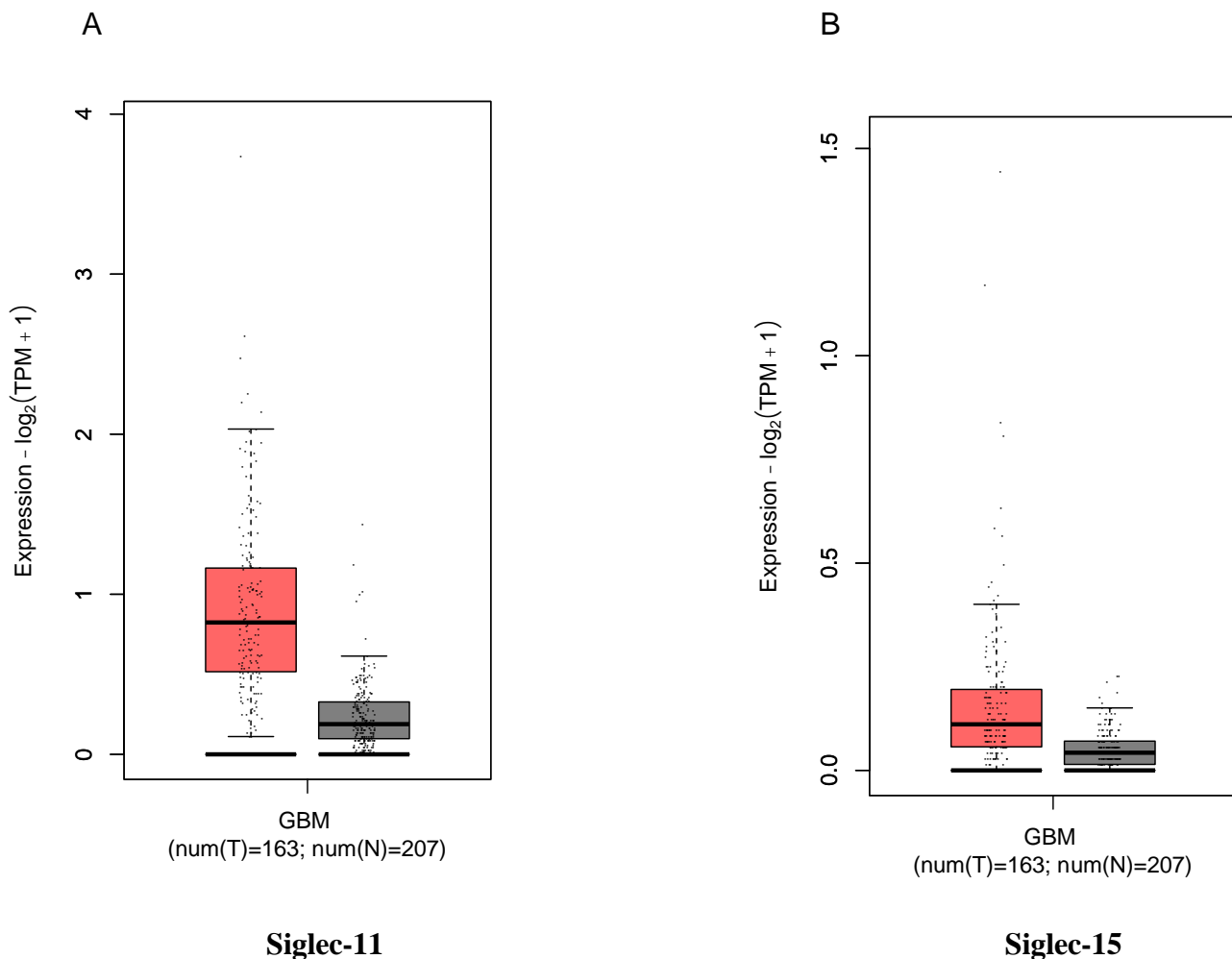


**Figure 7.** Expression analysis of chosen Siglecs using GEPIA. Siglec-11 and Siglec-15 were both upregulated in glioblastoma tumour samples (red) in comparison to normal brain tissue (grey). (A) Expression analysis of Siglec-11 of patients with GBM in red (n=163) compared to healthy patients in grey (207). (B) Expression analysis of Siglec-15 of patients with GBM in red (n=163) compared to healthy patients in grey (207).

The results from the bioinformatic analysis using GEPIA showed that Siglec-11 and Siglec-15 are highly upregulated in cancer patients. However, there was no statistical difference in the survival of glioblastoma patients between the high and low expressors of both chosen Siglecs.

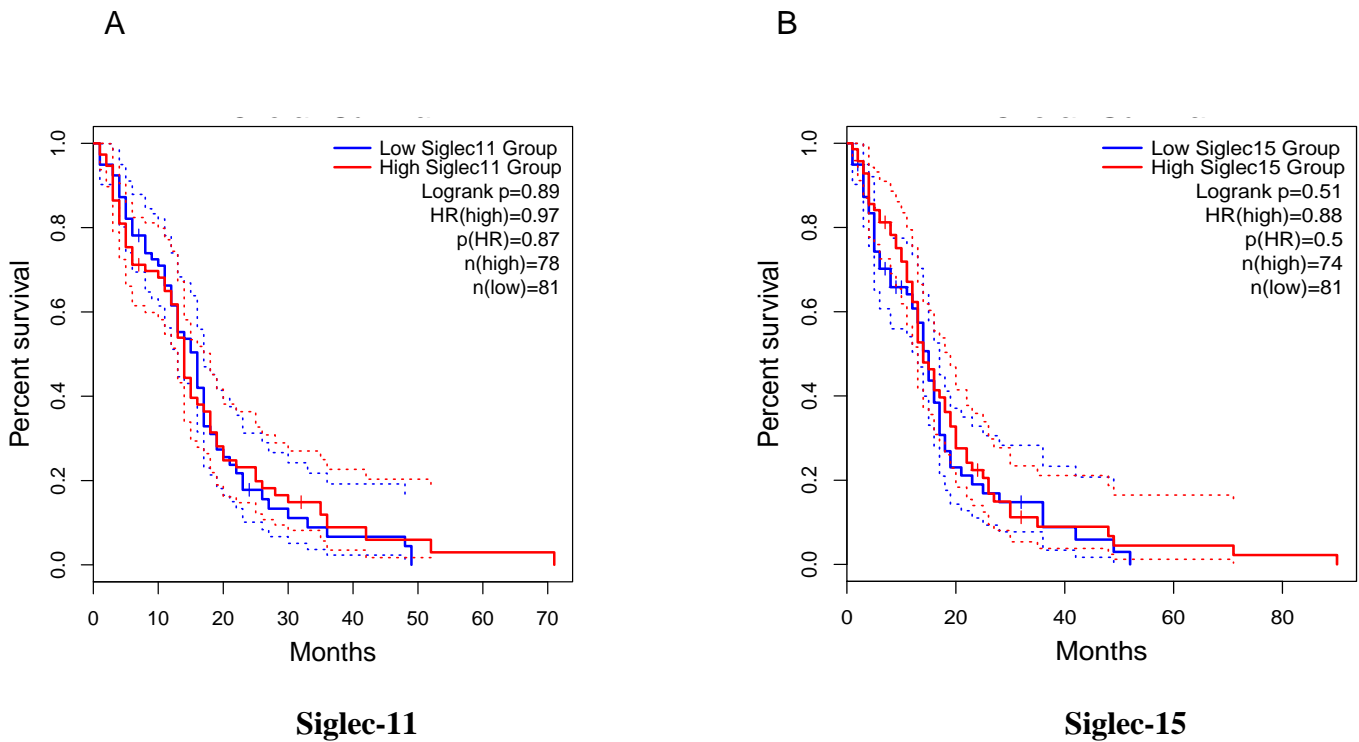
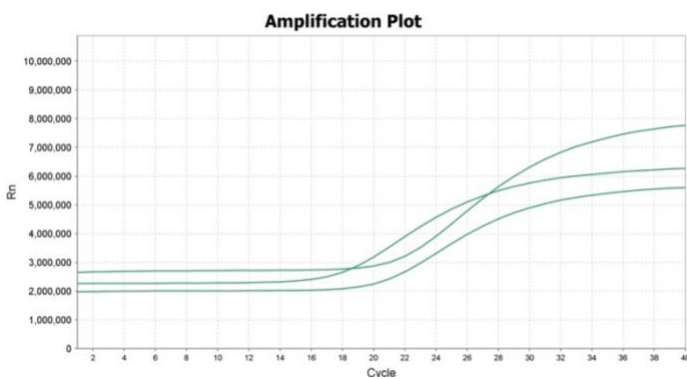


**Figure 8.** Overall survival analysis of chosen Siglecs using GEPIA. The survival percentage was compared between high and low expressors of Siglec-11 and Siglec-15 in cancer patients. (A) Overall survival analysis of high and low expressors of Siglec-11 in patients with GBM. (B) Overall survival analysis of high and low expressors of Siglec-15 in patients with GBM.

### 3.2 RT-qPCR results

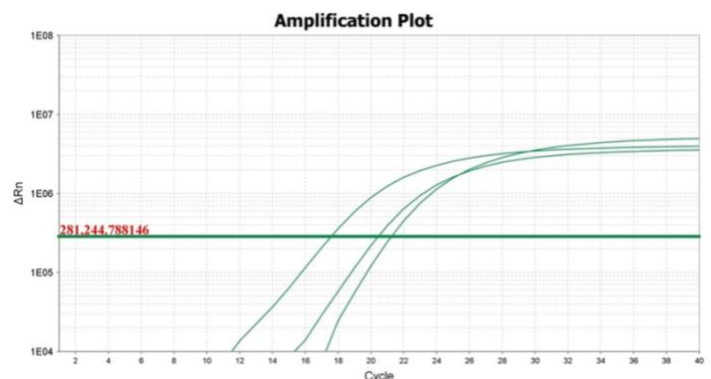
Figure 9 represents the results obtained with the A172 GBM cell line. Figure 9A1 and figure 9A2 show the linear and log plots for the control miRNA used, hsa-miR-RNU-44. The expression for this miRNA started between cycles 17 and 11. The expression of hsa-miR-138-5p in figure 9B1 and figure 9B2 started between cycles 19 and 21 which was slightly later than that shown in the control, indication that hsa-miR-138-5p is slightly under-expressed in comparison to the control miRNA, hsa-miR-RNU-44. Hsa-miR-153, shown in figure 9C1 and figure 9C2, started expressing between cycles 33 and 21, respectively. This expression is far later than that of the control which indicates that this miRNA is under-expressed in comparison. Finally, hsa-miR-107 (Figure 9, D1 and D2) started expressing between cycles 28 and 23, respectively. In comparison to the control miRNA, this indicates that the hsa-miR-107 is under-expressed.

A1



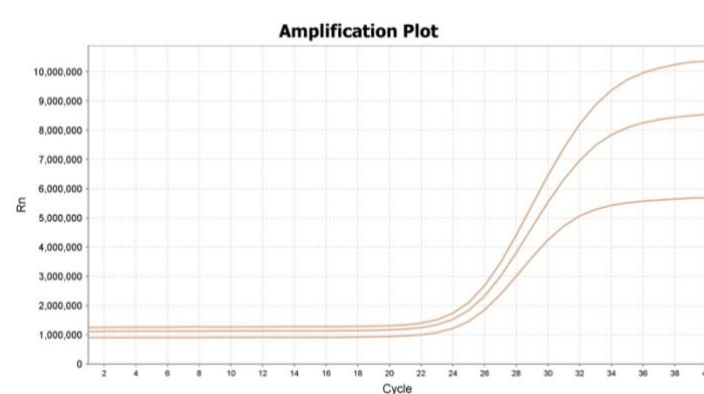
Hsa-miR-RNU-44

A2



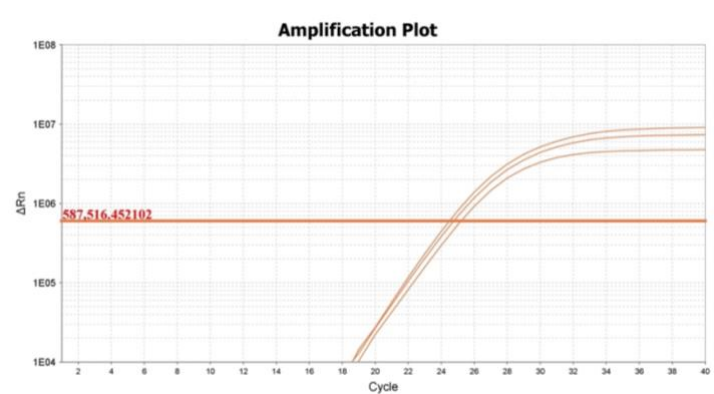
Hsa-miR-RNU-44

B1



Hsa-miR-138-5p

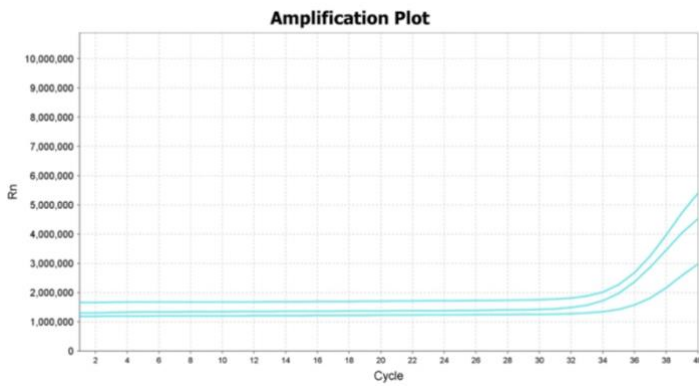
B2



Hsa-miR-138-5p

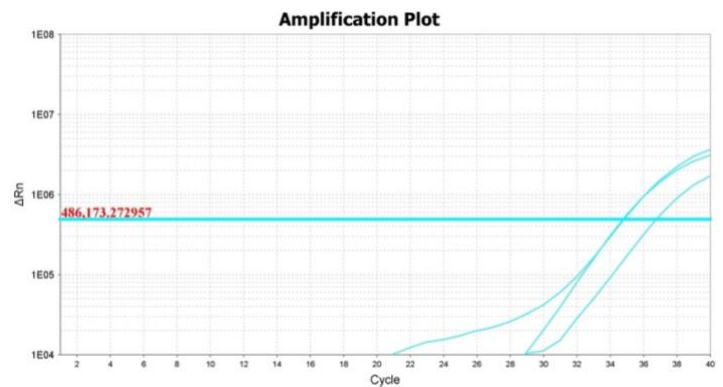
---

C1



Hsa-miR-153

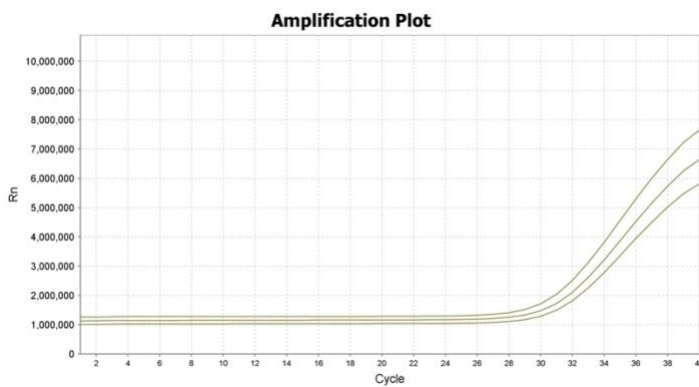
C2



Hsa-miR-153

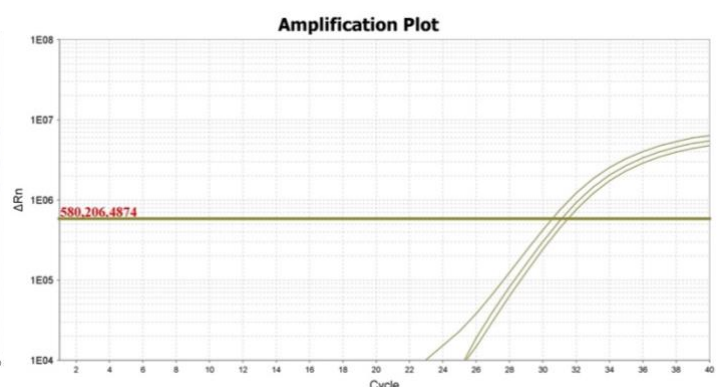
---

D1



Hsa-miR-107

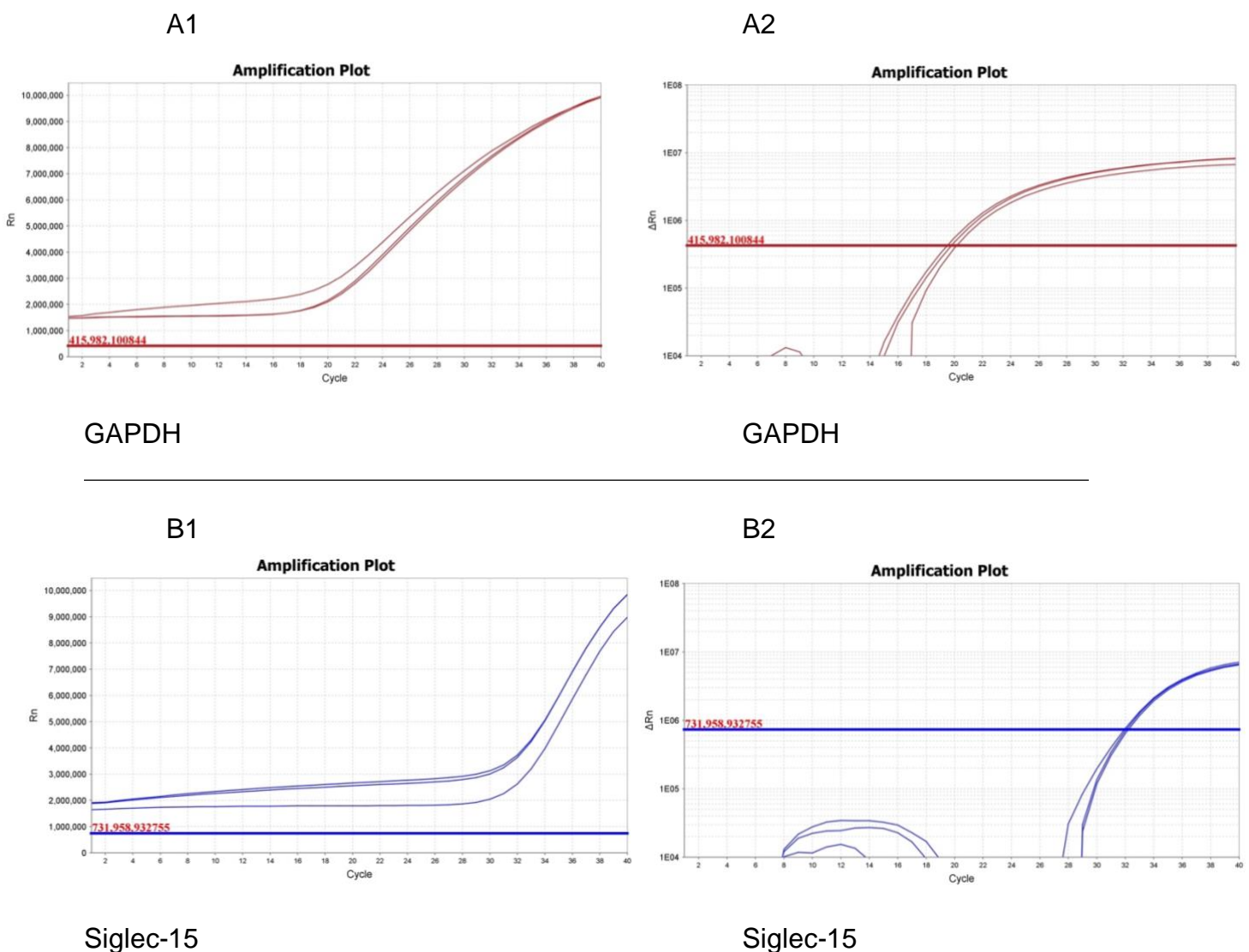
D2



Hsa-miR-107

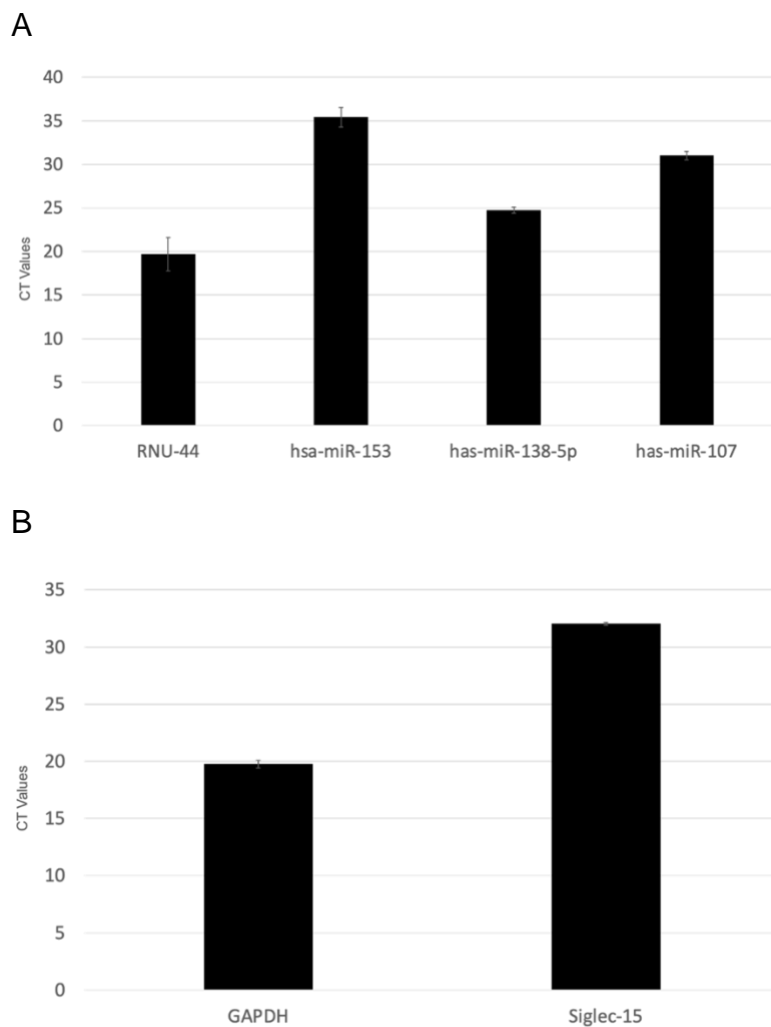
**Figure 9.** Linear and log amplification plots from RT-qPCR for hsa-miR-RNU-44, hsa-miR-138-5p, hsa-miR-153 and hsa-miR-107 within the A172 GBM cell line. The X-axis represents the linear plot (Rn) and the log plot ( $\Delta Rn$ ). The Y-axis represent the cycle number.

Figure 10 represents the results obtained with the A172 GBM cell line. Figure 10A1 and 10A2 show the linear and log plots for the control gene used, GAPDH. The expression for this gene started from the first cycle for the linear plot and from the 7<sup>th</sup> cycle for the log plot. The expression level started increasing from the 15<sup>th</sup> cycle onwards. Siglec-15 gene (figure 10B1 and figure 10B2) showed instant expression in the linear plot and expression from the 8<sup>th</sup> cycle for the log plot. This expression is later than the expression of the control which indicates that Siglec-15 is under-expressed in the A172 GBM cell line.



**Figure 10.** Linear and log amplification plots from RT-qPCR for Siglec-15 and GAPDH within the A172 GBM cell line. The X-axis represents the linear plot (Rn) and the log plot ( $\Delta Rn$ ). The Y-axis represent the cycle number.

Figure 11A. The CT value represents the threshold cycle value which is the value above which there us fluorescence seen beyond the background readings. MiRNA 153 has the highest CT values amongst the results thus indicating that this miRNA is highly downregulated. Similarly, miRNAs 107 and 138-5p also suggest down-regulation due to their CT values being higher than that of the control miRNA – RNU-44. In 11B, similar results are seen where the CT value is much higher than that of GAPDH.



**Figure 11.** CT values for RT-qPCR results of the following miRNAs: RNU-44, miR-153, miR-138-5p, miR-107 and the following genes: GAPDH and Siglec-15 in A172 cell line. The mean CT value was plotted, and the standard deviation is presented as error bars. The fold change of miRNA could not be obtained due to the lack of normal a normal brain cell line. However, the crude CT values for each miRNA is plotted.

### 3.3 Western blot results

In the A172 GBM cell line, 3 different markers were tested: Siglec-15, *E2F3* and *CDK6*. The theoretical molecular weight of these markers are as follows: 60-70 kDA, 60-65 kDA and 50-70 kDA. The weak bands that are present in figure 12 may be caused by an insufficient incubation time or due to the antibody being too dilute.

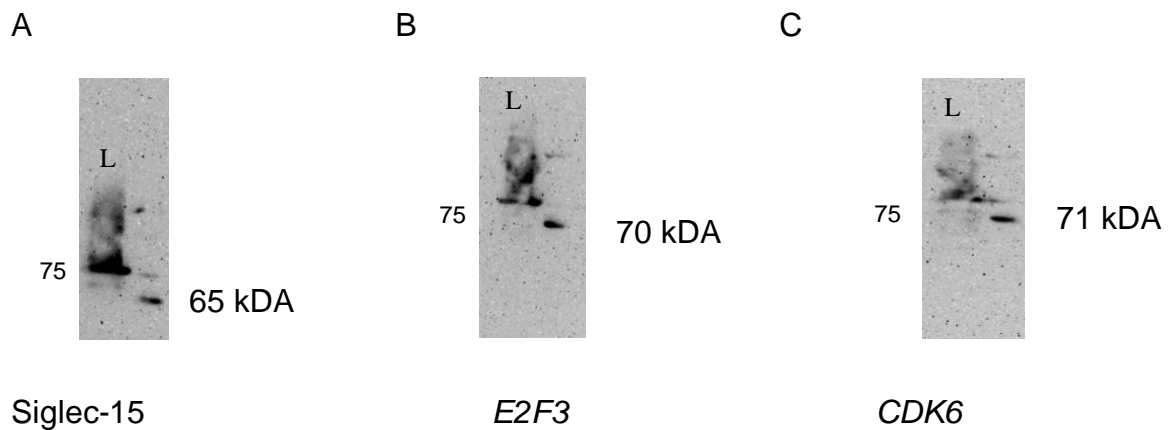


**Figure 12.** Western blot results for Siglec-15, *E2F3* and *CDK6* within the A172 GBM cell line. (A) Siglec-15 with observed molecular weight 65 kDA, L refers to the ladder. (B) *E2F3* with observed molecular weight of 70 kDA, L refers to the Ladder. (C) *CDK6* with observed molecular weight of 71 kDA, L refers to the ladder.

## 4. Discussion

Glioblastoma remains the most aggressive malignant tumour in adults. Despite developments in treatments and therapies, there is an absence of effective pharmacological and surgical therapies causing poor prognosis and low survival rates. Therefore, identifying early diagnostic and prognostic biomarkers is critical for improving patient survival rate and for developing novel treatments (Silantyev, A. et al. 2019). A systematic review by Møller H. *et al.* (2012) revealed that there are more than 300 miRNAs implicated in glioblastoma. Out of those 300 miRNAs, 253 are over-expressed and 95 are under-expressed. This includes hsa-miR-138-5p which has been found to be under-expressed in glioblastoma. MicroRNA expression patterns have been altered in neurodegenerative disorders, ischemic brain regions, and brain tumours. The greater understanding of microRNAs' function in disease, their influence on neuroprotection and neurogenesis, makes them a promising target for novel therapeutic applications (Godlewski, J. et al. 2019).

Expressed in tumour cells of various types of cancer, Siglec genes have been utilised by tumours to escape immune surveillance. The broad function of Siglec expression is not well understood, yet it is believed that it has the potential to play a vital role in the survival of cancer patients (Chen, Z. et al., 2020). It is shown that miRNA interact with Siglec genes by inhibiting their expression. The gene miR-215 directly binds to the 3'-UTR of Siglec-8, causing a cascade effect of suppressed cell migration and proliferation due to the diminishment of miR-215 (Lei, H. et al., 2016). From research, the correlation of Tumour-associated microglia (MG) and GBM cells during tumorigenesis has been studied by Tomás A. Martins and colleagues (2020) during immunotherapeutic clinical trials for the treatment of GBM as immunosuppressive MG was "the main factor for treatment failure". It was inferred by Tomás A. Martins and colleagues (2020) that the reason behind treatment failures is due to underestimating the counteracting contributions of immunosuppressive MG. This is supported by Lim, Sari-Ak, and Bagga (2021) as they concluded that tumour cells utilise immunosuppressants engagement along Siglec-sialic acid axis can cause suppression to immune response leading to tumour growth. Considering that Siglecs-sialic acid structures are in constant interaction in the tumour micro-environment, Siglecs are recognised at tumour cells' target to be able to control the effector cell-



signalling responses (Lim, J. et al. 2021). Understanding the immunosuppressive role of MG and its effects on Siglec-silica acid structures is complex and many new analytical techniques are being used to make new discoveries, enabling more effective treatment for cancer. Most Siglecs have an inhibitory effect due to the presence of the immunoreceptor tyrosine-based inhibitory motif (ITIM). An example of this would be Siglec-11, which is known as an inhibitory Siglec. However, some Siglecs including Siglec-15 and Siglec-16 interact with immune receptor tyrosine-based activating motifs (ITAM), such as DAP-10, and operate as activating molecules (Murugesan G. et al. 2021). The expression of Siglec-15 has been found in macrophages that are tumour-associated (Rashid S. et al. 2022).

MiRNA-138-5p acts as a tumour suppressor gene in glioblastoma by targeting CCND3 (a protein-coding gene), resulting in the suppression of tumour survival thus implying that this mRNA might be a viable diagnostic/therapeutic target for glioblastoma (Henggang Wu, et al. 2020). The expression of this miRNA is shown to be downregulated in glioblastoma (Margret Yeh, et al. 2019). This is also supported by figure 9 (part B1 and B2), where the miRNA was found to be slightly under-expressed when compared to the control (RNU-44).

The brain enriched miR-153 has been found to be a tumour suppressor in cancers such as osteosarcoma and non-small cell lung cancer (Liu, Z. et al. 2017). It has been found that miR-153 is abundantly expressed in the brain but is abnormally downregulated in GBM compared to normal brains, indicating that miR-153 may play an essential role in the progression of GBM (Toraih, E. et al. 2019). This finding is supported by figure 9 (part C1 and C2) where the expression of this miRNA was shown to be under-expressed compared to the control miRNA used in the A172 GBM cell line. Further studies have suggested that miR-153 promotes apoptosis and could restrain cell proliferation by suppressing the expression of B-cell lymphoma 2 (Bcl-2) (Xu, J. et al. 2011) which regulates the mitochondrial pathway of apoptosis by arresting cells in the G0 phase (Chipuk, J. et al. 2010).

MiRNA-107 has been established to be a glioma suppressor and its downregulation has been shown in gliomas, glioma cell lines and in glioma stem-like cells. This has been shown in figure 9D1 and figure 9D2 where the miRNA was under-expressed in

comparison to the control (RNU-44). It was discovered that hsa-miR-107 expression levels are lower in gliomas compared to normal brain and in high-grade gliomas compared to low-grade gliomas (Ji, Y. et al. 2015). Overexpression of this miRNA in glioma cells leads to the inhibition of proliferation, invasiveness and migration via targeting p53 and CDK6 (Hermansen, S. K. et al. 2017).

E2f transcription factors (E2Fs) are a family of transcription factors that play an important role in controlling cell cycle equilibrium. E2Fs are classified into three categories based on their structure and recognised function; this study focuses on the activators which include *E2F3*. Activators become more abundant at the G1-S transition, whereas atypical repressors surge in the late S phase (Yu, H. et al. 2020) In different types of malignancies, including brain and CNS tumours, the over expression of *E2F3* is considered as a tumour suppressor. For example, miR128-1 reduced GBM development by targeting *E2F3* and increased *E2F3a* expression was linked to the development of glioma. In a study that was conducted by Liao, P. et al. (2020) *E2F3* expression was shown to be increased in GBM. However, its expression and gene alterations in GBM have no association with overall survival outcomes. Furthermore, in GBM the expression of *E2F3* was found to be associated to tumour purity. As a result, *E2F3* represents a viable therapeutic target in patients with immune cell infiltration of GBM.

*CDK6* belongs to a family of serine/threonine kinase that regulate cell cycle progression by interacting with cyclin D and phosphorylating the retinoblastoma protein during the G1/S transition. Elevated *CDK6* protein expression has also been documented in GBM. MiRNAs are molecules that regulate protein creation by either blocking or suppressing the translation of target mRNA. These microRNAs control the production of signalling molecules such as cytokines, growth factors and transcription factors. Given that abnormally produced miRNAs can play important roles in the development of human malignancies, current research has focused on the potential therapeutic uses of these molecules (Garofalo M, et al. 2011). Both the loss and increase of miRNA function can lead to cancer formation by upregulating and silencing certain target genes, respectively. Correcting these miRNA dysregulations with miRNA antagonists or miRNA mimics might be a helpful therapeutic method for interfering with critical pathways implicated in cancer formation (Chen, S. et al. 2013).

## **5. Conclusion**

This research has shown the down-regulated expression of the following miRNAs in cancer; hsa-miR-138-5p, hsa-miR-153 and hsa-miR-107. These miRNAs were assessed within the GBM A172 cell line. The downregulation thus suggests that these miRNAs may manifest tumour suppressor properties. Siglec-11 and Siglec-15, which are regulated by tumour suppressor miRNAs, can be explored as diagnostic markers and therapeutic targets in GBM. However, before considering the use of Siglecs as therapeutics, it is necessary to further investigate the various functions of Siglecs based on their expression in different cell types.

## **6. Future work**

Bioinformatic analysis completed in this research has highlighted 3 main miRNAs that needed further investigation. Hsa-miR-485-5p, hsa-miR-138-5p and hsa-miR-10a-5p were present across all the bioinformatic tools used. The expression of these miRNAs needs to be tested in GBM cell lines and their expression compared to normal brain cell lines. This should also be carried out for the different markers used in western blotting. Future work should involve the comparison between the expression of the markers in a normal brain cell line and a GBM cell line in which transfection of miRNA mimics is involved.

## 7. References

- Preusser, M., De Ribaupierre, S., Wöhrer, A., Erridge, S. C., Hegi, M., Weller, M., & Stupp, R. (2011). Current concepts and management of glioblastoma. *Annals of neurology*, *70*(1), 9-21.
- Davis M. E. (2016). Glioblastoma: Overview of Disease and Treatment. *Clinical journal of oncology nursing*, *20*(5 Suppl), S2–S8. <https://doi.org/10.1188/16.CJON.S1.2-8>
- Jovčevska, I., Kočevsar, N., & Komel, R. (2013). Glioma and glioblastoma-how much do we (not) know? *Molecular and clinical oncology*, *1*(6), 935-941.
- Aldape, K., Zadeh, G., Mansouri, S., Reifenberger, G., & von Deimling, A. (2015). Glioblastoma: pathology, molecular mechanisms and markers. *Acta neuropathologica*, *129*(6), 829-848.
- Ohgaki, H., & Kleihues, P. (2007). Genetic pathways to primary and secondary glioblastoma. *The American journal of pathology*, *170*(5), 1445-1453.
- Birzu, C., French, P., Caccese, M., Cerretti, G., Idbaih, A., Zaganel, V., & Lombardi, G. (2020). Recurrent glioblastoma: from molecular landscape to new treatment perspectives. *Cancers*, *13*(1), 47.
- Tan, A. C., Ashley, D. M., López, G. Y., Malinzak, M., Friedman, H. S., & Khasraw, M. (2020). Management of glioblastoma: State of the art and future directions. *CA: a cancer journal for clinicians*, *70*(4), 299-312.
- Ostrom, Q. T., Gittleman, H., Farah, P., Ondracek, A., Chen, Y., Wolinsky, Y., ... & Barnholtz-Sloan, J. S. (2013). CBTRUS statistical report: Primary brain and central nervous system tumors diagnosed in the United States in 2006-2010. *Neuro-oncology*, *15*(suppl\_2), ii1-ii56.
- Tamimi, A. F., & Juweid, M. (2017). Epidemiology and outcome of glioblastoma. Exon Publications, 143-153.
- Alexander, B. M., & Cloughesy, T. F. (2017). Adult glioblastoma. *Journal of Clinical Oncology*, *35*(21), 2402-2409.
- Huang, B., Zhang, H., Gu, L., Ye, B., Jian, Z., Stary, C., & Xiong, X. (2017). Advances in immunotherapy for glioblastoma multiforme. *Journal of immunology research*, 2017.
- Brown, N. F., Carter, T. J., Ottaviani, D., & Mulholland, P. (2018). Harnessing the immune system in glioblastoma. *British journal of cancer*, *119*(10), 1171-1181.

Lee, D. H., Ryu, H. W., Won, H. R., & Kwon, S. H. (2017). Advances in epigenetic glioblastoma therapy. *Oncotarget*, 8(11), 18577.

Stupp, R., Hegi, M. E., Mason, W. P., Van Den Bent, M. J., Taphoorn, M. J., Janzer, R. C., ... & National Cancer Institute of Canada Clinical Trials Group. (2009). Effects of radiotherapy with concomitant and adjuvant temozolomide versus radiotherapy alone on survival in glioblastoma in a randomised phase III study: 5-year analysis of the EORTC-NCIC trial. *The lancet oncology*, 10(5), 459-466.

Gzell, C., Back, M., Wheeler, H., Bailey, D., & Foote, M. (2017). Radiotherapy in Glioblastoma: The Past, the Present and the Future. *Clinical Oncology*, 29(1), 15-25.

Paolillo, M., Boselli, C., & Schinelli, S. (2018). Glioblastoma under Siege: An Overview of Current Therapeutic Strategies. *Brain sciences*, 8(1), 15. <https://doi.org/10.3390/brainsci8010015>

Davis M. E. (2016). Glioblastoma: Overview of Disease and Treatment. *Clinical journal of oncology nursing*, 20(5 Suppl), S2–S8. <https://doi.org/10.1188/16.CJON.S1.2-8>

Shergalis, A., Bankhead, A., Luesakul, U., Muangsin, N., & Neamati, N. (2018). Current challenges and opportunities in treating glioblastoma. *Pharmacological reviews*, 70(3), 412-445.

Mc Adam, A. J., Schweitzer, A. N., & Sharpe, A. H. (1998). The role of B7 co-stimulation in activation and differentiation of CD4+ and CD8+ T cells. *Immunological reviews*, 165(1), 231-247.

Thomas, A. A., Ernstoff, M. S., & Fadul, C. E. (2012). Immunotherapy for the treatment of glioblastoma. *Cancer journal (Sudbury, Mass.)*, 18(1), 59.

Schraml, B. U., & e Sousa, C. R. (2015). Defining dendritic cells. *Current opinion in immunology*, 32, 13-20.

Wilcox, J. A., Ramakrishna, R., & Magge, R. (2018). Immunotherapy in glioblastoma. *World Neurosurgery*, 116, 518-528.

Kamran, N., Calinescu, A., Candolfi, M., Chandran, M., Mineharu, Y., Asad, A. S., ... & Castro, M. G. (2016). Recent advances and future of immunotherapy for glioblastoma. *Expert opinion on biological therapy*, 16(10), 1245-1264.

Sanders, S., & Debinski, W. (2020). Challenges to successful implementation of the immune checkpoint inhibitors for treatment of glioblastoma. *International Journal of Molecular Sciences*, 21(8), 2759.

S. Berghoff, B. Kiesel, G. Widhalm et al., "Programmed death ligand 1 expression and tumor-infiltrating lymphocytes in glioblastoma," *Neuro-Oncology*, vol. 17, no. 8, pp. 1064–1075, 2015.

Y. Liu, R. Carlsson, M. Ambjørn et al., "PD-L1 expression by neurons nearby tumors indicates better prognosis in glioblastoma patients," *The Journal of Neuroscience*, vol. 33, no. 35, pp. 14231–14245, 2013.

E. K. Nduom, J. Wei, N. K. Yaghi et al., "PD-L1 expression and prognostic impact in glioblastoma," *Neuro-Oncology*, vol. 18, no. 2, pp. 195–205, 2016.

Szopa, W., Burley, T. A., Kramer-Marek, G., & Kaspera, W. (2017). Diagnostic and therapeutic biomarkers in glioblastoma: current status and future perspectives. *BioMed research international*, 2017.

Majc, B., Novak, M., Jerala, N. K., Jewett, A., & Breznik, B. (2021). Immunotherapy of glioblastoma: current strategies and challenges in tumor model development. *Cells*, 10(2), 265.

Varki, A., & Angata, T. (2006). Siglecs—the major subfamily of I-type lectins. *Glycobiology*, 16(1), 1R-27R

Von Gunten, S., & Bochner, B. S. (2008). Basic and clinical immunology of Siglecs. *Annals of the New York Academy of Sciences*, 1143(1), 61-82.

Duan, S., & Paulson, J. C. (2020). Siglecs as immune cell checkpoints in disease. *Annual review of immunology*, 38, 365-395.

Wilky, B. A. (2019). Immune checkpoint inhibitors: the linchpins of modern immunotherapy. *Immunological reviews*, 290(1), 6-23.

Hayakawa, T., Khedri, Z., Schwarz, F., Landig, C., Liang, S. Y., Yu, H., ... & Angata, T. (2017). Coevolution of Siglec-11 and Siglec-16 via gene conversion in primates. *BMC evolutionary biology*, 17(1), 1-11.

Varki, A., & Gagneux, P. (2012). Multifarious roles of sialic acids in immunity. *Annals of the New York Academy of Sciences*, 1253(1), 16.

- Varki, A., Schnaar, R. L., & Schauer, R. (2017). Sialic acids and other nonulosonic acids. Essentials of Glycobiology [Internet]. 3rd edition
- Linnartz-Gerlach, B., Kopatz, J., & Neumann, H. (2014). Siglec functions of microglia. *Glycobiology*, 24(9), 794-799.
- Wang, Y., & Neumann, H. (2010). Alleviation of neurotoxicity by microglial human Siglec-11. *Journal of Neuroscience*, 30(9), 3482-3488.
- Angata, T. (2020). Siglec-15: A potential regulator of osteoporosis, cancer, and infectious diseases. *Journal of biomedical science*, 27(1), 1-7.
- Hong, S., You, J. Y., Paek, K., Park, J., Kang, S. J., Han, E. H., ... & Kim, J. A. (2021). Inhibition of tumor progression and M2 microglial polarization by extracellular vesicle-mediated microRNA-124 in a 3D microfluidic glioblastoma microenvironment. *Theranostics*, 11(19), 9687.
- Touat, M., Idbaih, A., Sanson, M., & Ligon, K. L. (2017). Glioblastoma targeted therapy: updated approaches from recent biological insights. *Annals of Oncology*, 28(7), 1457-1472.
- Huang, S., Shao, K., Liu, Y., Kuang, Y., Li, J., An, S., ... & Jiang, C. (2013). Tumor-targeting and microenvironment-responsive smart nanoparticles for combination therapy of antiangiogenesis and apoptosis. *ACS nano*, 7(3), 2860-2871.
- Padfield, E., Ellis, H. P., & Kurian, K. M. (2015). Current therapeutic advances targeting EGFR and EGFRvIII in glioblastoma. *Frontiers in oncology*, 5, 5.
- Xu, Y. Y., Gao, P., Sun, Y., & Duan, Y. R. (2015). Development of targeted therapies in treatment of glioblastoma. *Cancer biology & medicine*, 12(3), 223.
- Agarwal, V., Bell, G. W., Nam, J. W., & Bartel, D. P. (2015). Predicting effective microRNA target sites in mammalian mRNAs. *elife*, 4, e05005.
- Silantyevev, A. S., Falzone, L., Libra, M., Gurina, O. I., Kardashova, K. S., Nikolouzakis, T. K., ... & Tsatsakis, A. (2019). Current and future trends on diagnosis and prognosis of glioblastoma: from molecular biology to proteomics. *Cells*, 8(8), 863.
- Toraih, E. A., Aly, N. M., Abdallah, H. Y., Al-Qahtani, S. A., Shaalan, A. A., Hussein, M. H., & Fawzy, M. S. (2017). MicroRNA–target cross-talks: Key players in glioblastoma multiforme. *Tumor Biology*, 39(11), 1010428317726842.



Quan, Y., Song, Q., Wang, J., Zhao, L., Lv, J., & Gong, S. (2017). MiR-1202 functions as a tumor suppressor in glioma cells by targeting Rab1A. *Tumor Biology*, 39(4), 1010428317697565.

Wang, C., Chen, Q., Li, S., Li, S., Zhao, Z., Gao, H., ... Zhong, J. (2016). Dual inhibition of PCDH9 expression by miR-215-5p up-regulation in gliomas. *Oncotarget*, 8(6), 10287–10297.  
<https://doi.org/10.18632/oncotarget.14396>

Vychytilova-Faltejskova, P., Merhautova, J., Machackova, T., Gutierrez-Garcia, I., Garcia-Solano, J., Radova, L., ... & Slaby, O. (2017). MiR-215-5p is a tumor suppressor in colorectal cancer targeting EGFR ligand epiregulin and its transcriptional inducer HOXB9. *Oncogenesis*, 6(11), 1-14.

Micolucci, L., Akhtar, M. M., Olivieri, F., Rippo, M. R., & Procopio, A. D. (2016). Diagnostic value of microRNAs in asbestos exposure and malignant mesothelioma: systematic review and qualitative meta-analysis. *Oncotarget*, 7(36), 58606.

Wu, H., Wang, C., Liu, Y., Yang, C., Liang, X., Zhang, X., & Li, X. (2020). miR-138-5p suppresses glioblastoma cell viability and leads to cell cycle arrest by targeting cyclin D3. *Oncology Letters*, 20(5), 1-1.

Yeh, M., Oh, C. S., Yoo, J. Y., Kaur, B., & Lee, T. J. (2019). Pivotal role of microRNA-138 in human cancers. *American journal of cancer research*, 9(6), 1118.

Liu, L., Zhu, Z., Li, X., & Zheng, Y. (2020). DNA methylation regulates glioma cell cycle through down-regulating MiR-133a-5p expression.

Zheng, L., Kang, Y., Zhang, L., & Zou, W. (2020). MiR-133a-5p inhibits androgen receptor (AR)-induced proliferation in prostate cancer cells via targeting FUsed in Sarcoma (FUS) and AR. *Cancer biology & therapy*, 21(1), 34-42.

Fujita, K., Iwama, H., Sakamoto, T., Okura, R., Kobayashi, K., Takano, J., ... & Masaki, T. (2015). Galectin-9 suppresses the growth of hepatocellular carcinoma via apoptosis in vitro and in vivo. *International journal of oncology*, 46(6), 2419-2430.

Fricke, A., Ullrich, P. V., Heinz, J., Pfeifer, D., Scholber, J., Herget, G. W., ... & Braig, D. (2015). Identification of a blood-borne miRNA signature of synovial sarcoma. *Molecular cancer*, 14(1), 1-13.

Li, J., Liu, X., Wang, W., & Li, C. (2020). miR-133a-3p promotes apoptosis and induces cell cycle arrest by targeting CREB1 in retinoblastoma. *Archives of medical science: AMS*, 16(4), 941.

Chang, L., Lei, X., Qin, Y. U., Zhang, X., Jin, H., Wang, C., ... & Su, J. (2015). MicroRNA-133b inhibits cell migration and invasion by targeting matrix metalloproteinase 14 in glioblastoma. *Oncology letters*, 10(5), 2781-2786.

Yu, J., Wu, S. W., & Wu, W. P. (2017). A tumor-suppressive microRNA, miRNA-485-5p, inhibits glioma cell proliferation and invasion by down-regulating TPD52L2. *American journal of translational research*, 9(7), 3336.

Worst, T. S., Previti, C., Nitschke, K., Diessl, N., Gross, J. C., Hoffmann, L., ... & Boutros, M. (2020). miR-10a-5p and miR-29b-3p as extracellular vesicle-associated prostate cancer detection markers. *Cancers*, 12(1), 43.

Ru, Q., Li, W. L., Xiong, Q., Chen, L., Tian, X., & Li, C. Y. (2018). Voltage-gated potassium channel blocker 4-aminopyridine induces glioma cell apoptosis by reducing expression of microRNA-10b-5p. *Molecular biology of the cell*, 29(9), 1125-1136.

Qian, M., Chen, Z., Guo, X., Wang, S., Zhang, Z., Qiu, W., ... & Li, G. (2021). Exosomes derived from hypoxic glioma deliver miR-1246 and miR-10b-5p to normoxic glioma cells to promote migration and invasion. *Laboratory Investigation*, 101(5), 612-624.

Dai, S., Wang, X., Li, X., & Cao, Y. (2015). MicroRNA-139-5p acts as a tumor suppressor by targeting ELTD1 and regulating cell cycle in glioblastoma multiforme. *Biochemical and biophysical research communications*, 467(2), 204-210.

Yue, S., Wang, L., Zhang, H., Min, Y., Lou, Y., Sun, H., ... & Li, Y. (2015). miR-139-5p suppresses cancer cell migration and invasion through targeting ZEB1 and ZEB2 in GBM. *Tumor Biology*, 36(9), 6741-6749.

Møller, H., Rasmussen, A., Andersen, H., Johnsen, K., Henriksen, M., & Duroux, M. (2012). A systematic review of microRNA in glioblastoma multiforme: micro-modulators in the mesenchymal mode of migration and invasion. *Molecular neurobiology*, 47(1), 131-144.

Chen, Z., Yu, M., Guo, L., Zhang, B., Liu, S., Zhang, W., ... & Ye, Q. (2020). Tumor derived SIGLEC family genes may play roles in tumor genesis, progression, and immune microenvironment regulation. *Frontiers in Oncology*, 10, 586820.

Lei, H., Li, H., Xie, H., Du, C., Xia, Y., & Tang, W. (2016). Role of MiR-215 in Hirschsprung's Disease Pathogenesis by Targeting SIGLEC-8. *Cellular Physiology and Biochemistry*, 40(6), 1646–1655. <https://doi.org/10.1159/000453214>

Lim, J., Sari-Ak, D., & Bagga, T. (2021). Siglecs as Therapeutic Targets in Cancer. *Biology*, 10(11), 1178. <https://doi.org/10.3390/biology10111178>

Martins, T. A., Schmassmann, P., Shekarian, T., Boulay, J.-L., Ritz, M.-F., Zanganeh, S., Hutter, G. (2020). Microglia-Centered Combinatorial Strategies Against Glioblastoma. *Frontiers in Immunology*, 11. <https://doi.org/10.3389/fimmu.2020.571951>

Godlewski, J., Lenart, J., & Salinska, E. (2019). MicroRNA in brain pathology: Neurodegeneration the other side of the brain cancer. *Non-coding RNA*, 5(1), 20.

Mao, H., LeBrun, D. G., Yang, J., Zhu, V. F., & Li, M. (2012). Deregulated signaling pathways in glioblastoma multiforme: molecular mechanisms and therapeutic targets. *Cancer investigation*, 30(1), 48-56.

Tortosa, A., Ino, Y., Odell, N., Swilley, S., Sasaki, H., Louis, D. N., & Henson, J. W. (2000). Molecular genetics of radiographically defined de novo glioblastoma multiforme. *Neuropathology and applied neurobiology*, 26(6), 544-552.

Aldape, K., Zadeh, G., Mansouri, S., Reifenberger, G., & von Deimling, A. (2015). Glioblastoma: pathology, molecular mechanisms and markers. *Acta neuropathologica*, 129(6), 829-848.

Lieberman, F. (2017). Glioblastoma update: molecular biology, diagnosis, treatment, response assessment, and translational clinical trials. *F1000Research*, 6.

Toraih, E. A., El-Wazir, A., Abdallah, H. Y., Tantawy, M. A., & Fawzy, M. S. (2019). Deregulated microRNA signature following glioblastoma irradiation. *Cancer Control*, 26(1), 1073274819847226

Liu, Z., Wang, J., Li, Y., Fan, J., Chen, L., & Xu, R. (2017). MicroRNA-153 regulates glutamine metabolism in glioblastoma through targeting glutaminase. *Tumor Biology*, 39(2), 1010428317691429.

Xu, J., Liao, X., Lu, N., Liu, W., & Wong, C. W. (2011). Chromatin-modifying drugs induce miRNA-153 expression to suppress Irs-2 in glioblastoma cell lines. *International journal of cancer*, 129(10), 2527-2531.

Chipuk, J. E., Moldoveanu, T., Llambi, F., Parsons, M. J., & Green, D. R. (2010). The BCL-2 family reunion. *Molecular cell*, 37(3), 299-310.

- Wu, H., Wang, C., Liu, Y., Yang, C., Liang, X., Zhang, X., & Li, X. (2020). miR-138-5p suppresses glioblastoma cell viability and leads to cell cycle arrest by targeting cyclin D3. *Oncology letters*, 20(5), 1-1.
- Yeh, M., Oh, C. S., Yoo, J. Y., Kaur, B., & Lee, T. J. (2019). Pivotal role of microRNA-138 in human cancers. *American journal of cancer research*, 9(6), 1118.
- Ji, Y., Wei, Y., Wang, J., Ao, Q., Gong, K., & Zuo, H. (2015). Decreased expression of microRNA-107 predicts poorer prognosis in glioma. *Tumor Biology*, 36(6), 4461-4466.
- Hermansen, S. K., Sørensen, M. D., Hansen, A., Knudsen, S., Alvarado, A. G., Lathia, J. D., & Kristensen, B. W. (2017). A 4-miRNA signature to predict survival in glioblastomas. *PLoS one*, 12(11), e0188090.
- Murugesan, G., Correia, V. G., Palma, A. S., Chai, W., Li, C., Feizi, T., ... & Crocker, P. R. (2021). Siglec-15 recognition of sialoglycans on tumor cell lines can occur independently of sialyl Tn antigen expression. *Glycobiology*, 31(1), 44-54.
- Rashid, S., Song, D., Yuan, J., Mullin, B. H., & Xu, J. (2022). Molecular structure, expression, and the emerging role of Siglec-15 in skeletal biology and cancer. *Journal of Cellular Physiology*, 237(3), 1711-1719.
- Yu, H., Li, Z., & Wang, M. (2020). Expression and prognostic role of E2F transcription factors in high-grade glioma. *CNS neuroscience & therapeutics*, 26(7), 741-753.
- Liao, P., Han, S., & Qu, H. (2020). Expression, prognosis, and immune infiltrates analyses of E2Fs in human brain and CNS cancer. *BioMed Research International*, 2020.
- Chen, S. M., Chen, H. C., Chen, S. J., Huang, C. Y., Chen, P. Y., Wu, T. W. E., ... & Wei, K. C. (2013). MicroRNA-495 inhibits proliferation of glioblastoma multiforme cells by downregulating cyclin-dependent kinase 6. *World journal of surgical oncology*, 11(1), 1-8.
- Garofalo, M., & Croce, C. M. (2011). microRNAs: Master regulators as potential therapeutics in cancer. *Annual review of pharmacology and toxicology*, 51, 25-43.

